BASE STATION BASEBAND DIGITAL PROCESSING IN NEXT GENERATION CDMA SYSTEMS

by

Li Yang Pan

A thesis submitted to the

Department of Electrical and Computer Engineering

in conformity with the requirements

for the degree of Master of Science (Engineering)

Queen's University

Kingston, Ontario, Canada

November, 1999

Abstract

A method for combining digital beamforming and power control in the downlink of a direct sequence code division multiple access system is first presented. The algorithm does not require the use of a downlink pilot signal to estimate the channel response vector (CRV) for each user. This CRV-based power control algorithm is comprised of three steps: (1) minimum mean-squared error channel estimation, (2) beamforming, and (3) optimum intra-cell power allocation. Using this CRV-based power control algorithm the coverage and capacity of a downlink system employing multiple antenna elements at the base station is studied in the presence of inter-cell and intra-cell interference. The results show that to achieve a -5 dB uncoded SINR, CRV-based power control would allow a five element base station antenna array to reduce base station density by a factor of four over that of a single antenna system.

The second contribution of this thesis is a proposed computationally efficient wideband CDMA spatial-temporal RAKE receiver structure. The receiver employs sequential decision-making as well as tree search techniques to significantly reduce computational requirements with only a small sacrifice in optimum performance. The computational complexity and SNR performance of the new structure is studied

through numerical calculations and simulation. The results show an 84% savings in computation can be achieved compared to a full search RAKE receiver structure with a performance degradation of only 0.9 dB.

Acknowledgements

First, I would like to thank my advisor, Professor Steven Blostein for the support and guidance throughout this research. Special thanks to Natural Science and Engineering Research Council, Queen's University and Prof. Blostein for the generous financial support. I would also like to thank my parents, who has shown great confidence in me and supported me throughout my academic career. I would also like to thank the members of the IPCL who has been very helpful in my studies. Finally I would like to thank Sheryl, who has provided me with continual emotional support and encouragement.

Contents

List of Tables

List of Figures

Symbols and Abbreviations

$\mathbf{a}_i$	channel response vector for a user i
$\mathbf{a}_{ij}$	channel response vector for the j^{th} path of user i
a_G	decision threshold for deciding if a signal is present or not
ADC	analoge to digital Converter
b	ratio of probability of missed detection and one minus probability of false alarm
$b_i(n)$	the data bit transmitted for user i at time n
$c_i(n)$	the pseudo noise sequence for user i at time n
CDMA	code division multiple access
CRV	channel response vector
CSI	channel state information
FDD	frequency division duplex
G	number of chips per symbol
$I_{N\times N}$	identity matrix of size $N \times N$
I_i	interference experienced by user i for downlink

IN_{ij}	interference plus noise for the i^{th} path of user i for uplink
MAI	multiple access interference
MC-CDMA	multi-carrier code division multiple access
MMSE	minimum mean squred error
$N(\mu, \sigma^2)$	normal distribution with mean μ and variance σ^2
P_D	probability of detection
P_M	probability of missed detection
P_F	probability of false alarm
PN	pseudo noise
QoS	quality of service
RMS	Root Mean Square
SINR	signal to interference noise ratio
SNR	signal to noise ratio
SPRT	sequential probability ratio test
TDD	time division duplex
Z_{ijk}	correlation statistic for the j^{th} path of the i^{th} user for the k^{th} sector
Z_{ij}	time domain correlation statistic for the j^{th} path of the i^{th} user
α_{ij}	scalar antennuation experienced by the j^{th} path of the i^{th} user

Chapter 1

Introduction

1.1 Motivation

There has been a tremendous increase in the demand for mobile wireless services. The bandwidth and time slot available for wireless applications are limited resources. To use these limited resources, various multiple access algorithms have been developed to facilitate the sharing of bandwidth and time slots. Early wireless services provide multiple access by dividing up the time slot for each user using TDMA (time division multiple access). Another multiple access method is to divide the frequency band into different slots using FDMA (frequency division multiple access). Direct Sequence Code Division Multiple Access (DS-CDMA) technology has provided an efficient means to provide multiple access to a high number of users without dividing the available resources into frequency or time slots by assigning to each user a pseudo-random code.

In the next generation of mobile phone products, new applications such as interactive multimedia and internet browsers will enhance functionality. These new applications for wireless mobile phones demand higher signal quality and bandwidth for the wireless link. To accommodate the increased demand, the base station must be able to provide enough signal quality to all users. The use of base station antenna arrays with half-wavelength inter-element spacing has been proposed to increase capacity. To achieve the high bandwidth necessary for wideband applications, multipath diversity can be used to increase system performance. In wideband CDMA (W-CDMA) proposals, the chip rates are five, ten or fifteen times the current IS-95 standard chip rate [1] [9] [26], such as the case of the NTT experiments of 1.92 mega-bits-per-second (Mbps) data transmissions using 15.36 mega-chips-per-second (Mcps) [27]. Experimental test system used in [40] used 5.1Mcps. The increased chip rate of wideband CDMA applications allows for finer resolutions on multipath signal components. At the same time, the number of possible multipath components also increases due to the smaller chip period.

We first present a channel estimation algorithm based on a Kalman filter is presented for the downlink channel with multiple antenna elements at the base station, and only one antenna element at the mobile. The channel estimation algorithm allows for dynamic estimation of the channel response vector (CRV) for the downlink channel utilizing minimal computational resources at the mobile station. The downlink beamformed channel utilizes a power allocation method presented by Yang and Xu [51] in conjunction with our proposed Kalman filter-based channel estimator. Our

performance results show that the estimation converges to the optimum estimator in the minimum mean squared error sense. The benefits of utilizing spatial diversity through the use of multiple element antenna arrays with half-wavelength inter-element spacing.

We then present a novel RAKE receiver structure for wideband CDMA environments where there is a high chip rate and a time-varying multipath channel, which makes fine time-resolution signal tracking impractical. In wideband CDMA, the number of multipath components can be large, and variable, with large delay spread in terms of the number of chips. A parallel adaptive network of RAKE fingers is proposed corresponding to all possible delay shifts and users. For wideband CDMA, the receiver's oversampling rate is lower than in IS-95 systems, such as in [27] where 2 times oversampling is used for a 15Mcps chip rate. Lower oversampling would limit the ability to perform fine multipath tracking using early-late algorithm [52]. Using a sequential detection scheme, only viable fingers above a signal power threshold are used to generate the output decision statistic. Combined with a spatial domain search for the best set beamforming weights, we demonstrate that we can implement a spatial-temporal RAKE (2-D RAKE) receiver with greatly reduced computation at the expense of only modest performance loss.

1.2 Summary of Contributions

The contributions of this thesis for the downlink channel are listed below:

- A minimum mean-squared error channel estimation algorithm is presented for transmission beamforming in the downlink channel with multiple antenna elements at the base station and one element at the mobile station without the use of pilot channels.

- A channel delay spread model is used to analytically determine intra-cell interference for a CDMA system synchronized to a dominant path.

- The power allocation algorithm presented by Yang and Xu in [51] is extended to include quality of service for different mobile stations.

- The coverage and capacity is determined for a multi-cell multi-user downlink system employing multiple antenna elements at the base station in the presence of inter-cell and intra-cell interference.

The contributions pertaining to the uplink channel are listed below:

- A wideband CDMA spatial-temporal RAKE receiver utilizing sequential detection and spatial tree search is presented for the uplink base station processing.

- A new algorithm was presented to calculate the performance of a sequential detector with dependent samples arising from tree search.

- The computational complexity and SNR performance of a system utilizing a 2-D RAKE uplink receiver is studied.

1.3 Thesis Outline

There are two main components in this thesis. The first component is a study of the downlink CDMA channel. The second component is a presentation of a new implementation of 2-D RAKE wideband CDMA receiver.

In Chapter 3, our downlink channel model is presented. Interference from within the cell (intra-cell interference) is included in our channel model. A channel estimation algorithm is presented, followed by a downlink transmission beamforming algorithm.

Using the model and algorithm presented in Chapter 3, performance evaluation is presented in Chapter 4. The channel estimation algorithm's performance is examined numerically using the numerical solution to the Riccati equation. The estimation error was also studied using simulation. Using Monte Carlo integration, the overall system capacity and coverage performance with a varying number of antenna elements at the base station is studied in the presence of interference from surrounding cells and from multiple access interference due to the delay spread from within the cell. The effect of having multiple cellular service levels on the SINR performance was also studied.

In Chapter 5, a new wideband CDMA 2-D RAKE receiver implementation is presented. The sequential detection is used as well as a tree-structured spatial search. A method for designing the sequential detector is developed. The computational requirements and overall performance of this 2-D RAKE receiver are also presented.

Chapter 2

Previous Work

There has been extensive previous research on the analysis of CDMA system performance for the uplink and temporal RAKE receivers. Previous research on downlink CDMA system performance and temporal-spatial RAKE receiver implementation for the uplink is limited. In this chapter, we will examine the most relevant references from the literature.

2.1 Downlink CDMA Processing Using Coherent Antenna Arrays

One of the contributions of this thesis is the study of the downlink CDMA processing and its effects in a frequency division duplex CDMA (FDD-CDMA) system using an antenna array with phase coherent signal processing. There has been some work on the assignment of power levels to users for time division duplex (TDD) systems

using coherent antenna array signal processing and in single antenna systems [51] [19]. To find the channel information in FDD systems, probing using a pilot signal was introduced by Gerlach [13], but in this work, a recursive algorithm is used to track the channel information without the use of a pilot signal. The recursive algorithm can effectively track the changes in the channel information in a dynamic environment. The performance of the channel estimation algorithm is studied in a multi-cell multi-user environment.

In the downlink channel for CDMA systems, since the base station has to transmit to all users simultaneously, the signal processing at the base station is more difficult to perform as well as analyze. To the best knowledge of the author, the performance of the downlink channels in CDMA systems has not been previously investigated.

Yang and Xu [51] have analyzed the problem of optimum power assignment assuming known directional beamforming weights in a TDD system. In [51], Yang and Xu used the array response vectors (steering) from the uplink channel as spatial directional beamforming weights in their algorithm. Since the channel response is a function of frequency [13], in FDD systems, the uplink channel response is different than the downlink channel response, resulting in the need for a channel estimation algorithm, see Figure 2.1. Other optimum power assignment algorithms were presented by Kim [19], Rashid-Farrokhi and Liu [12] in the cases where there is no beamforming is performed at the base station.

For FDD systems, Gerlach [13] proposed in to estimate the channel response

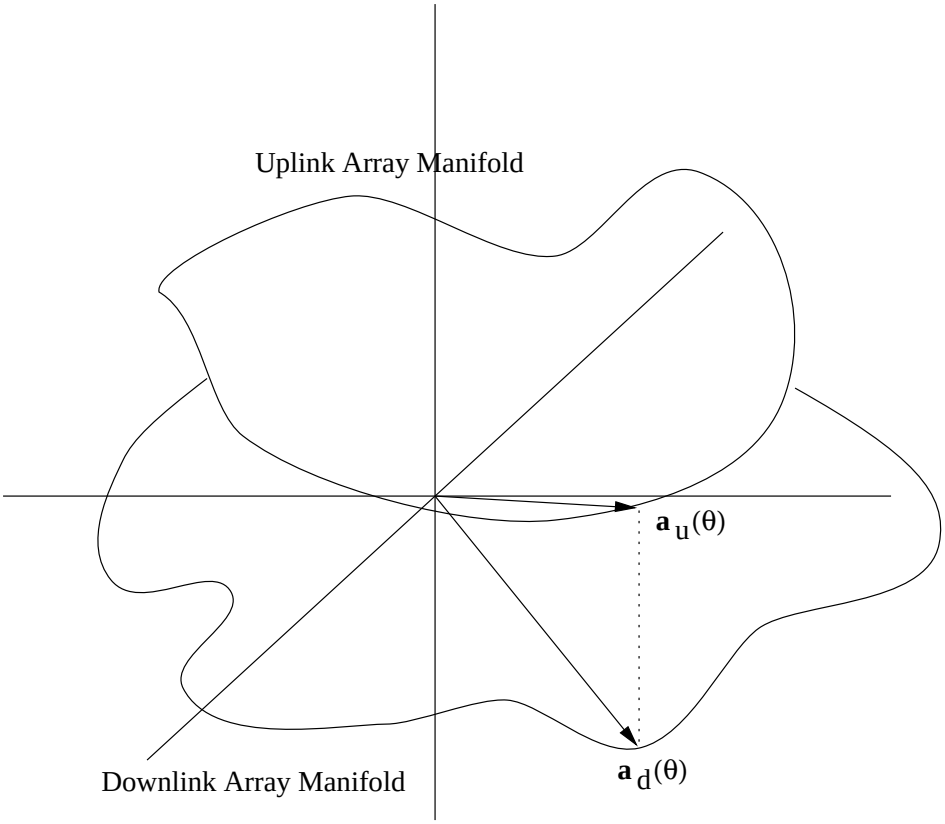

Figure 2.1: Array manifold is dependent on frequency. For FDD systems, uplink and downlink manifolds are different

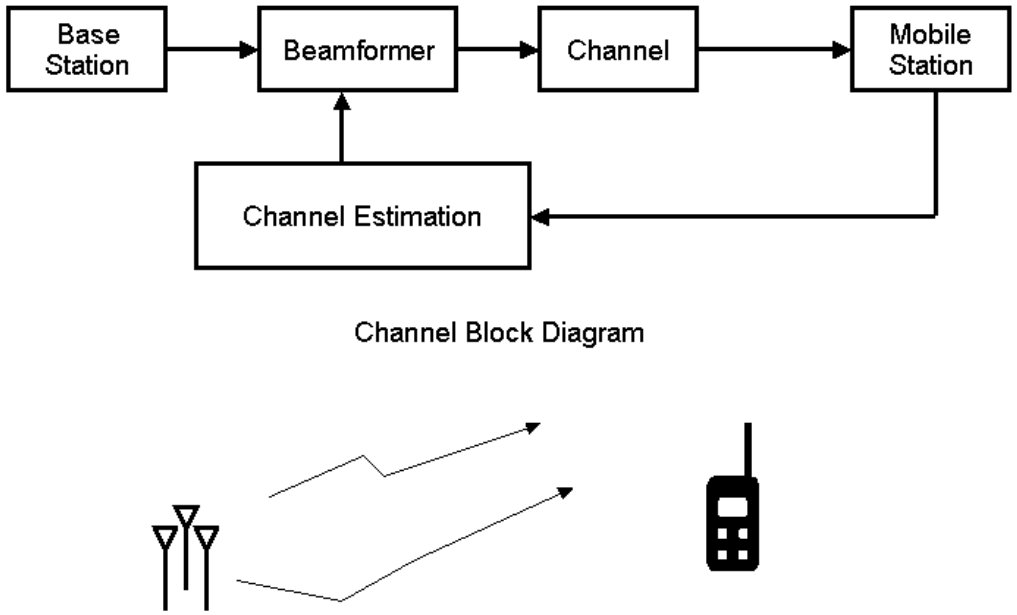

Figure 2.2: Downlink system block diagram representation in a multipath environment

for the downlink channel using a pilot signal transmitted by each antenna. The received signal strength is fed back to the base station and used for determining the beamforming weights. In Chapter 3, the proposed algorithm for downlink channel estimation does not use pilot signals. The system block diagram for the downlink is shown in Figure 2.2.

2.2 RAKE Processing for CDMA Uplink Channel

A block diagram model of the traditional temporal CDMA RAKE receiver can be found in the [33] (See Figure 2.3). In the diagram, T_c is the chip rate, T is the symbol

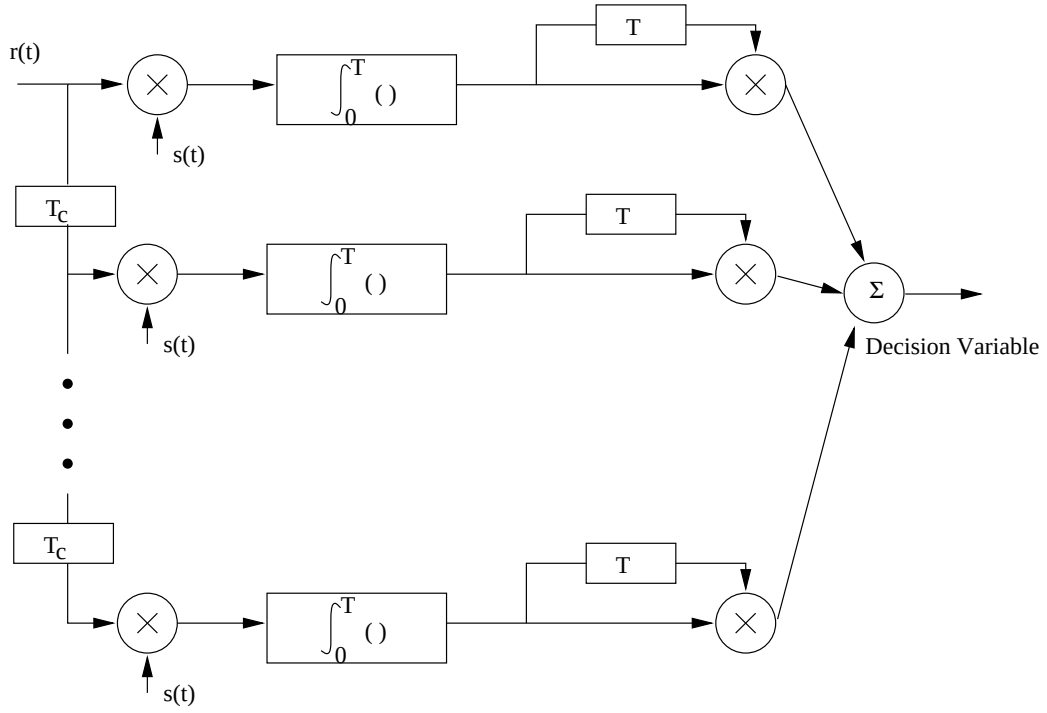

Figure 2.3: RAKE demodulator for DPSK signals

period and $s(t)$ is the modulating waveform.

Previous references on RAKE receivers dealt with time domain implementations where there was no beamforming performed at the receiver. A detailed analysis of the RAKE receiver can be found in Proakis [33]. Recently, Naguib and Paulraj introduced the concept of a 2D-RAKE receiver utilizing both spatial and temporal characteristics of the multipath channel[23].

In the 2D-RAKE receiver proposed by Naguib and Paulraj [23], a different beamformer was to be used for each possible delay shift. If the resulting statistic, $z_l(n)$, is greater than a threshold, a beamforming weight and delay pair is used for RAKE combining. Otherwise no signal is assumed present for that particular delay (See

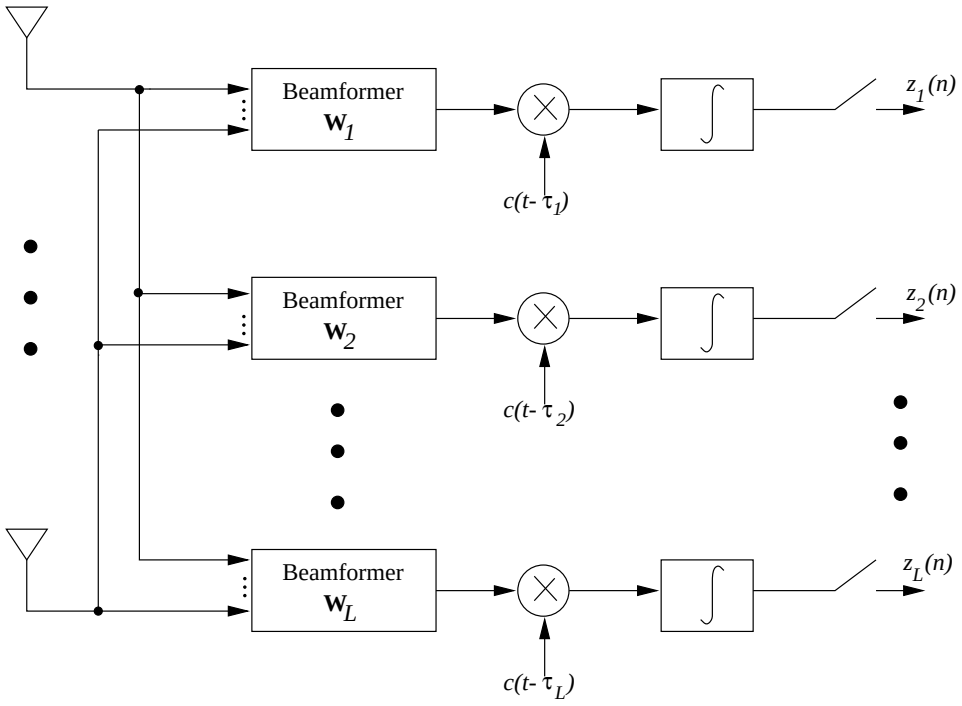

Figure 2.4: Space-Time Matched Filter proposed by Naguib and Paulraj

Figure 2.4). In Figure 2.4, w_l is the beamforming weight for the l^{th} delay and $\tilde{c}$ is the PN code for a particular user.

An alternative to direct sequence CDMA (DS-CDMA) for wideband CDMA is multi-carrier CDMA (MC-CDMA). In MC-CDMA, the transmitted signal is passed through a serial-to-parallel multiplexer, and sent over several channels, each with lower bandwidth. Each channel in MC-CDMA has a smaller chip rate than in wideband DS-CDMA, resulting in a smaller number of resolvable paths. The smaller number of resolvable paths reduces the need for many RAKE fingers, thereby reducing complexity. Although more difficult to implement than, the performance of DS-CDMA has been shown to be superior to that of MC-CDMA [16]. The amount

of performance gain for using DS-CDMA is dependent on the multipath scenario. In [18], Kim and Cho studied the capacity improvements using an antenna array for MC-CDMA, but the results do not incorporate multipath effects, nor do they propose how to effectively estimate the beamforming weights for each carrier. The additional computational complexity required to implement a beamformer for each carrier has not been studied. Further research is necessary to compare MC-CDMA and DS-CDMA performance.

In conventional CDMA, a special PN acquisition algorithm is used to search for the correct shift in PN code. In the search for the correct shift, a PN acquisition algorithm must search through a large search space. In multipath situations, the multipath components are shifted within a finite interval relative to the dominant path, resulting in a much smaller search space. In RAKE reception, it is often assumed we know the maximum delay of multipath components relative to the dominant path.

2.3 Application of Sequential Detection in CDMA Systems

For a CDMA system, there is negligible correlation between signals separated by over one chip period. Therefore, to correctly match the relative delay between the generated PN sequence at the receiver and the received signal, search is required. Most multi-dwell detectors use several decision stages to detect whether the correct

delay is achieved. If not, the delay is rejected, and the search is performed again for the next delay in a serial fashion [52]. Detailed studies of PN acquisition can be found in [39] and [52].

Sequential detectors were first introduced by Wald [45]. It has been proven that the sequential probability ratio test results in minimum average detection time for a specified probability of detection and false alarm [46]. In [39] and [52] sequential detection is referred to as the most sophisticated type of PN acquisition algorithm. In [41], a comprehensive study of optimum threshold selection for sequential detectors in traditional PN acquisition applications are presented. In [15], a sequential PN acquisition algorithm is designed and is shown to outperform non-sequential acquisition algorithms.

After the signal is acquired, a tracking algorithm using an early-late structure is often used to track the delay of the PN sequence to achieve the highest correlation with the received signal space [52]. The use of the early-late structure requires oversampling of the received chips. For wideband CDMA system the oversampling rate is small [27]. In [27], the sampling rate is 4 times the chip rate using a 8-bit analog to digital converters (ADC) allowing tracking to within plus or minus one quarter of a chip. Higher oversampling rates for wideband CDMA are impractical due to the cost of implementing very high speed ADCs.

In this thesis, the focus is on wideband CDMA systems where one of the dominant paths is assumed known. A search is performed over many adjacent delay intervals for

multipath energy. Since the search space comprises a large number of chips, a sequential detection algorithm is particularly well-suited to achieve coarse PN acquisition. The resulting statistic from the PN acquisition stage can be made the same as the correlation statistic from the matched filter, and can be used for RAKE combining. A further stage of spatial search will assign the optimum beamforming weights from a pre-calculated set to the multipaths.

Chapter 3

Downlink Channel Model and Beamforming

3.1 Introduction

The benefits of CDMA [9] [10] [34] have enabled increased capacity in cellular networks. The use of antenna arrays with inter-element spacing of less than half a wavelength has been proposed to further increase the capacity of CDMA by utilizing the frequency re-use made possible by the spatial separation of mobiles. The effect of antenna arrays on uplink beamforming performance has been well-studied in recent years [8] [11] . For the downlink, the research has not been as extensive. Inherent differences exist between the uplink and downlink channels. In the uplink, the base station can process individual users' signals separately and in parallel. Significant resources are available at the base station to process the incoming signals. For

the downlink, the base stations transmit to all users simultaneously, and the mobile stations have restrictions on computational resources. The signals to different users interfere with one another because they all share the same frequency band and time slots. In a conventional single-user receiver based system, the capacity of the system is determined by the amount of multiple access interference (MAI)[14]; therefore, it is important to minimize the amount of MAI in a CDMA system. The use of orthogonal codes effectively eliminates MAI within a cell if there is no multipath in the channel. However, the reduction of MAI due to users from other cells cannot be addressed with orthogonal codes, since the codes are reused for each cell, and the base stations do not transmit with the same propagation delay to a particular mobile. In realistic environments, MAI exists within the cell due to multipath, because multipath components arrive asynchronously, and therefore are not orthogonal to the dominant signal component.

For conventional single-user receivers, for each user, energy from all users is received and chip-matched filters are employed to despread the desired user's signal. Thus, interfering signals are seen by the receiver as MAI. To ensure that the link quality is above some minimum level, the signal to interference plus noise ratio (SINR) must be above some threshold [12]. Since the transmitted power of the base station is limited, the total power transmitted to all users is constrained. In order to maximize the SINR, the total transmitted power should be the same as the maximum power of the transmitter. If system is not power controllable, regardless of the power available at the base station, we cannot guarantee a particular service level for all users. The

reason that some systems are not power controllable is that these systems are interference limited. In a system where the SINR has been maximized and the resulting SINR is lower than the desired level, even if the total transmitter power is increased, the SINR for individual users cannot be increased. Any additional power to increase a user's SINR will result in additional interference for other users, generating more interference for the original user. If the maximum SINR that can be achieved is below the minimum requirements for a particular data rate, then the system is not power controllable.

In the case where antenna arrays are utilized, spatial separation of mobile stations allows the base station to decrease the MAI by adjusting the directional gain for each user's signal. Array signal processing, which occurs digitally and at baseband, can be made transparent to existing CDMA systems. In this thesis, we assume that digital beamforming is applied to the baseband signal.

In this chapter, we construct a model of the downlink transmission channel in a synchronous CDMA (S-CDMA) system utilizing antenna arrays. A least squares based channel estimation method is proposed to estimate the channel response vectors (CRV), without the use of a downlink training sequence, or special downlink pilot channels such as those proposed by Gerlach and Paulraj [13]. The proposed algorithm uses a scalar feedback from the mobile to perform channel estimation, downlink beamforming and power allocation. The proposed algorithm performs CRV-based power control for the downlink.

3.2 Motivation

In Yang and Xu, [51], a method of maximizing the minimum SINR is given. In order to find the weights to obtain the optimum SINR, the channel response vectors (CRVs) must be known. Generally, the CRV for the uplink and downlink channels are different for FDD systems. Therefore, the uplink channel state information (CSI) cannot be substituted for the downlink CSI. Gerlach and Paulraj proposed the use of probing signals to estimate the CRV in [13]. Probing signals are transmitted during a training period, or "probe mode", and CSI is then fed back to the base station via a separate channel. We propose to estimate the CRV without the use of probing signals by using the transmitted bits to estimate the CRV. In addition, only a scalar signal strength value is fed back to the base station by each mobile. The proposed method therefore utilizes less protocol overhead by avoiding the "probe mode", as well as reducing the amount of information collected and fed back to the base station (i.e. feedback bandwidth).

With the knowledge of the CRV at the base station, we can power control to maximize the SINR for each user in the cell. The proposed CRV-based power control algorithm consists of three steps, CRV estimation, generating directional beamforming weight vectors and allocate power for each user in the cell.

3.3 Channel Model

In our downlink channel model, we assumed that an M-element array is used at the base station for transmission beamforming serving N mobile users in the cell, who simultaneously share the same bandwidth and time slots, using direct-sequence CDMA. The mobile is assumed to have only one antenna in this study, which is consistent with low-cost user terminals.

The baseband expression for the superposition of signals transmitted by the k^{th} base station $\mathbf{x}_k(t)$ can be written as:

$$\mathbf{x}_k(t) = \sum_{i=1}^{N} \mathbf{w}_{ik} s_{ik}(t) \qquad k = 1, ..., K \tag{3.1}$$

where, $s_{ik}(t)$ is the signal for the i^{th} user in cell k, and $\mathbf{w}_{ik}$ is set of antenna weights for the i^{th} user in the k^{th} cell.

Assuming we have a synchronous downlink channel (the synchronous assumption for systems such as IS-95 hold true in practice [49]). We also assume that the receiver has locked onto the dominant path. For simplicity, we assume that the number of users is the same in each cell included in our calculations. Without loss of generality, we assume the first cell is the cell of interest. Therefore the transmitted signal for the cell of interest is $\mathbf{x}_1$. The signal received by the j^{th} mobile user in the first cell is:

$$y_j(t) = \mathbf{a}^*_{j,1,1}\mathbf{x}_1(t) + \sum_{l=2}^{L} \mathbf{a}^*_{j,l,1}\mathbf{x}_1(t - \tau_{j,l,1}) + \sum_{k=2}^{K}\sum_{l=1}^{L} \mathbf{a}^*_{j,l,k}\mathbf{x}_k(t - \tau_{j,l,k}) + n_j(t) \tag{3.2}$$

where $\mathbf{a}_{j,l,k}$ is the CRV for the l^{th} path for the j^{th} mobile in the k^{th} cell, and $n_j(t)$ is additive noise seen by the j^{th} user. Superscript $*$ denotes conjugate transpose. The

CRV comprises of the overall effects of path loss, shadowing and fading. The quantity $\tau_{i,l,k}$ is the relative delay between the l^{th} path of the base station in the k^{th} cell and the dominant path of the j^{th} user.

We also assume that the CRV is changing slowly with respect to the symbol period. This assumption is needed in order to be able to estimate the CRV and update the CRV for transmission beamforming at a later time at the base station.

The received signal $y_j(t)$ contains the desired signal and the interference plus noise. We use orthogonal codes in synchronous CDMA. The interference power, I_i can be written as:

$$I_i = \| \sum_{l=2}^{l=L} \mathbf{a}^*_{i,l,1} \mathbf{x}_1(t - \tau_{i,l,1}) + \sum_{k=2}^{k=K} \sum_{l=1}^{l=L} \mathbf{a}^*_{i,l,k} \mathbf{x}_k(t - \tau_{i,l,k}) \|^2 \tag{3.3}$$

Due to orthogonality between users for the dominant signal, no interference from the signal destined for other users in the dominant path will be experienced by the i^{th} mobile. The signal power for the i^th user is:

$$S_i = \|\mathbf{a}^*_{i,1,1} \mathbf{s}_{11}(t)\|^2 \tag{3.4}$$

where $\mathbf{s}_{11}(t)$ is the transmitted signal for user 1 in the first cell.

To simplify the notation, denote, the CRV for the dominant path to each user in the center cell from the center base station as

$$\mathbf{a}_i = \mathbf{a}_{i,1,1} \tag{3.5}$$

The CRV $\mathbf{a}_i$ can be separated into a directional component $\mathbf{v}_i$ and an attenuating

factor α_i. The relationship between them are:

$$\mathbf{v}_i = \frac{\mathbf{a}_i}{\|\mathbf{a}_i\|^2} \tag{3.6}$$

$$\alpha_i = \|\mathbf{a}_i\|^2 \tag{3.7}$$

where $\mathbf{v}_i$ is the normalized CRV, containing only the directional information of the i^{th} path, and α_i is the attenuation factor for the i^{th} path.

In a synchronous CDMA system with data rate R, and bandwidth W, we can write the SNR at the i^{th} mobile as given by Gilhousen et. al., in [14]:

$$SNR_i = \left(\frac{E_b}{N_0}\right)_i = \frac{S_i}{I_i + \sigma^2}\frac{W}{R} \tag{3.8}$$

The interference experienced at the i^{th} mobile contains power from all the base stations operating at the same frequency and time. Therefore, in a CDMA system, a user will experience both intra-cell and inter-cell interference. As the distance increases from the user, the interference power is reduced exponentially due to path-loss. We assume, for simplicity, that for a hexagonal cell layout where only the 18 surrounding cells (2 rings of cells) contribute to intercell interference. The base station configuration is shown in Fig. 3.1.

The proposed algorithm for CRV-based power control consists of three separate steps:

1) The CRV is estimated using a recursive estimator based on a Kalman filter.

2) The transmission directional weights are generated using the CRV.

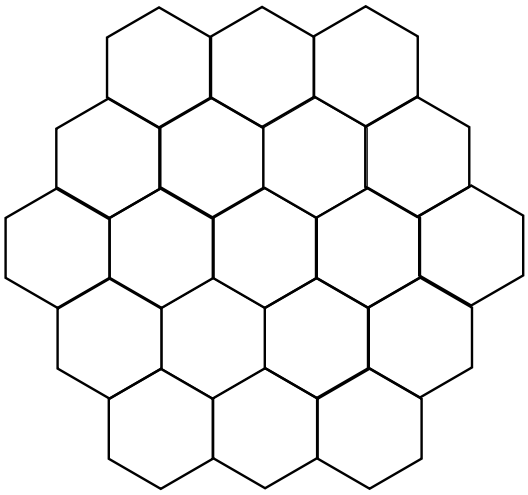

Figure 3.1: Layout of the hexagonal cells.

3) Power is allocated to each user to maximize the SINR.

A method for estimating the CRV is first examined. We will then briefly review the power allocation method outlined in [51], assuming we know the CRV and the normalized directional beamforming weights. The power allocation method is generalized to include users with varying desired uncoded SNR. Finally, we will examine two methods to find the normalized directional beamforming weights. Each step will now be discussed in detail.

3.4 Channel Estimation

Algorithms for beamforming generally require the knowledge of the CRV for each of the users within the cell. Gerlach and Paulraj have proposed a CRV estimation technique in [13], using probing signals. The use of probing signals requires protocol

overhead. There are two modes of operation, probing mode and information mode. In the probing mode, the signal strength from each antenna element is measured and fed back to the base station. Thus an additional protocol is required to decide when to switch modes.

Alternatively, to estimate the CRVs we can use the information bits known at the base station, as training sequences. At each mobile, the received signal power is fed back to the base station, and the feedback signal is then used to estimate the CRV using a least-squares method. We can use either a batch model estimation of CRV or a recursive estimation based on a Kalman filter. The knowledge of the CRV is used for beamforming and power allocation later in the algorithm, therefore a separate power control algorithm is not needed.

The total transmitted digital signal from the base station at time n is:

$$\mathbf{x}(n) = \sum_{i=1}^{N} \mathbf{w}_i d_i(n) \tag{3.9}$$

where $\mathbf{w}_i$ is the beamforming weight vector for user i, and $d_i(n)$ is the n^{th} bit for user i.

The received value at mobile k at time n is:

$$y_k(n) = \mathbf{x}^T(n)\mathbf{a}_k(n) + I_k(n) + n_k(n) \tag{3.10}$$

Note that the k^{th} mobile receives a superposition of signals that are being broadcast to all users from the base station.

If we make the assumption that only the direct path power from each of the eighteen interfering base stations will contribute interference power to the mobile, we

can analytically calculate the noise power from each interfering base station if the beamforming weights are known.

3.4.1 Interference from Surrounding Base Stations

In this section, we will derive the average interference power including the effects of shadowing and path loss. We assume we have flat (frequency-nonselective) fading, and that the average fading level is unity and is independent of shadowing and path loss. The effects of shadowing and path-loss is also assumed to be independent.

First, let the i^{th} base station be located at distance B_i, with an angle ϑ_i, with respect to due east of the base station. We denote the corresponding cartesian coordinates as Bx_i and By_i, respectively. They are related by:

$$Bx_i = B_i cos(\vartheta) \tag{3.11}$$

$$By_i = B_i sin(\vartheta) \tag{3.12}$$

$$Bx_i^2 + By_i^2 = B_i \tag{3.13}$$

The average power loss between the mobile located at (x, y) (or (r, θ) in polar coordinates) in the center cell and the i^{th} base station can be calculated as follows:

$$PL_i = G_i(r, \theta)((x - Bx_i)^2 + (y - By_i)^2)^{\frac{-\epsilon}{2}} 10^{\frac{\xi}{10}} \tag{3.14}$$

where ϵ denotes the path-loss exponent and has a typical value of 4 for urban environment; ξ is normally distributed with mean zero, and variance σ_S^2. The standard deviation σ_S has a typical value of 8 dB. $G_i(r, \theta)$ denotes the directional gain for the

power transmitted by the i^{th} base station to the mobile located at (r, θ) in the center cell. The value of the directional gain is dependent on the beamforming patterns and the location of mobile station.

The average interference for a mobile located in the center cell with cell radius R, assuming a uniform distribution, is:

$$E\{PL_i\} = \int_0^R \int_0^{2\pi} \frac{1}{2\pi R^2} G_i(r,\theta)((rcos(\theta) - Bx_i)^2 + (rsin(\theta) - By_i)^2)^{\frac{-\epsilon}{2}} E\{10^{\frac{\xi}{10}}\} r dr d\theta \tag{3.15}$$

The expected value of the effect of shadowing can be found as follows:

$$\begin{aligned} E\{10^{\frac{\xi}{10}}\} &= \int_{-\infty}^{\infty} 10^{\frac{\xi}{10}} e^{\frac{\xi^2}{2\sigma_S^2}} d\xi & (3.16)\\ &= \int_{-\infty}^{\infty} e^{\frac{\xi}{10}\log(10)} e^{\frac{\xi^2}{2\sigma_S^2}} d\xi & (3.17)\\ &= \int_{-\infty}^{\infty} e^{\frac{(\xi + \frac{\sigma_S^2}{10}\log(10))^2}{2\sigma_S^2} + \frac{\sigma_2}{200}\log(10)^2} d\xi & (3.18)\\ &= e^{\frac{\sigma_S^2}{200}\log(10)^2} & (3.19) \end{aligned}$$

where "log" denotes the natural logarithm in the above equations.

Therefore, the mean power loss from the i^{th} base station to a mobile in the center cell is:

$$E\{PL_i\} = \frac{1}{2\pi R^2} e^{\frac{\sigma_S^2}{200} log(10)^2} \int_0^R \int_0^{2\pi} G_i(r,\theta)((rsin(\theta) - Bx_i)^2 + (rsin(\theta) - By_i)^2)^{\frac{-\epsilon}{2}} r d\theta dr \tag{3.20}$$

The mean for the path-loss exponent of 4 is:

$$E\{PL_i\} = e^{\frac{\sigma_S^2}{200} log(10)^2}$$

$$\int_0^R \int_0^{2\pi} \{G_i(r,\theta)(r^2 cos^2(\theta) + Bx_i^2 - 2Bx_i r cos(\theta)$$

$$+ r^2 sin^2(\theta) + By_i^2 - 2By_i r sin(\theta))^{-2}\} r dr d\theta \quad (3.21)$$

$$= e^{\frac{\sigma_S^2}{200} log(10)^2} \int_0^{2\pi} \int_0^R G_i(r,\theta) \frac{r}{(r^2 + B_i^2 - 2B_i r cos(\theta - \vartheta))^2} d\theta dr \quad (3.22)$$

No closed form solution exists for the above integral. The average power loss can be found instead using numerical methods.

The actual interference experienced at the mobile will also depend on the directional gain of transmission beamforming, which will depend on the location of mobiles within each of the interfering cells. In the next chapter, numerical integration results are provided to examine this interference in various scenarios.

3.4.2 Downlink Intra-cell Interference due to Local Scatterers

At a particular frequency, the RMS delay spread is assumed to be constant. The effect of RMS delay on the interference created is chip-rate dependent. As the chip rate increases, more of the scatterers will be more than one chip period away from the dominant path. Therefore, the interference created by local scatterers will also increase.

To be consistent with observations of experimental data [35], we model the power spread as exponentially distributed. If the RMS delay spread is σ_τ, and $P(\tau)$ denotes the power received at that delay, expressed as a fraction of the dominant path energy.

The distribution of the power is then:

$$P(\tau) = \begin{cases} e^{-\frac{\tau^2}{2\sigma_\tau^2}} & \text{if } \tau \geq 0 \\ 0 & \text{if } \tau < 0 \end{cases} \tag{3.23}$$

With the use of orthogonal codes for downlink channel, the transmitted signals for each user have zero cross correlation. If shifted versions of signals are created by multipath are no longer orthogonal [33], and square transmission pulses are used to modulate orthogonal PN sequences, then the cross correlation energy between different orthogonal codes can be expressed as [10] [33],

$$E_{multipath}(\tau) = Var\{c_i(t)c_j(t-\tau)\} \tag{3.24}$$

$$= \begin{cases} \frac{\tau^2}{T_c^2} & \text{for } |\tau| \leq T_c \\ 1 & \text{otherwise} \end{cases} \tag{3.25}$$

where T_c is the chip period, and $c_i(t)$ is the PN code the i^{th} user.

Therefore, as the multipath delay exceeds the chip period, the interference caused by the multipath component is identical to the multipath interference experienced when using non-orthogonal PN sequences. The interference energy as a function of multipath delay τ is, using (3.23) and (3.25)

$$P_I(\tau) = \begin{cases} P(\tau)\frac{\tau^2}{T_c^2} & \text{for } \tau \in [0,T_c] \\ P(\tau) & \text{for } \tau > T_c \\ 0 & \text{for } \tau < 0 \end{cases} \tag{3.26}$$

where T_c is the chip rate.

In Fig. 3.2, the intra-cell interference power as a fraction of the dominant path power, is plotted as a function of RMS delay for three different chip rates. The use

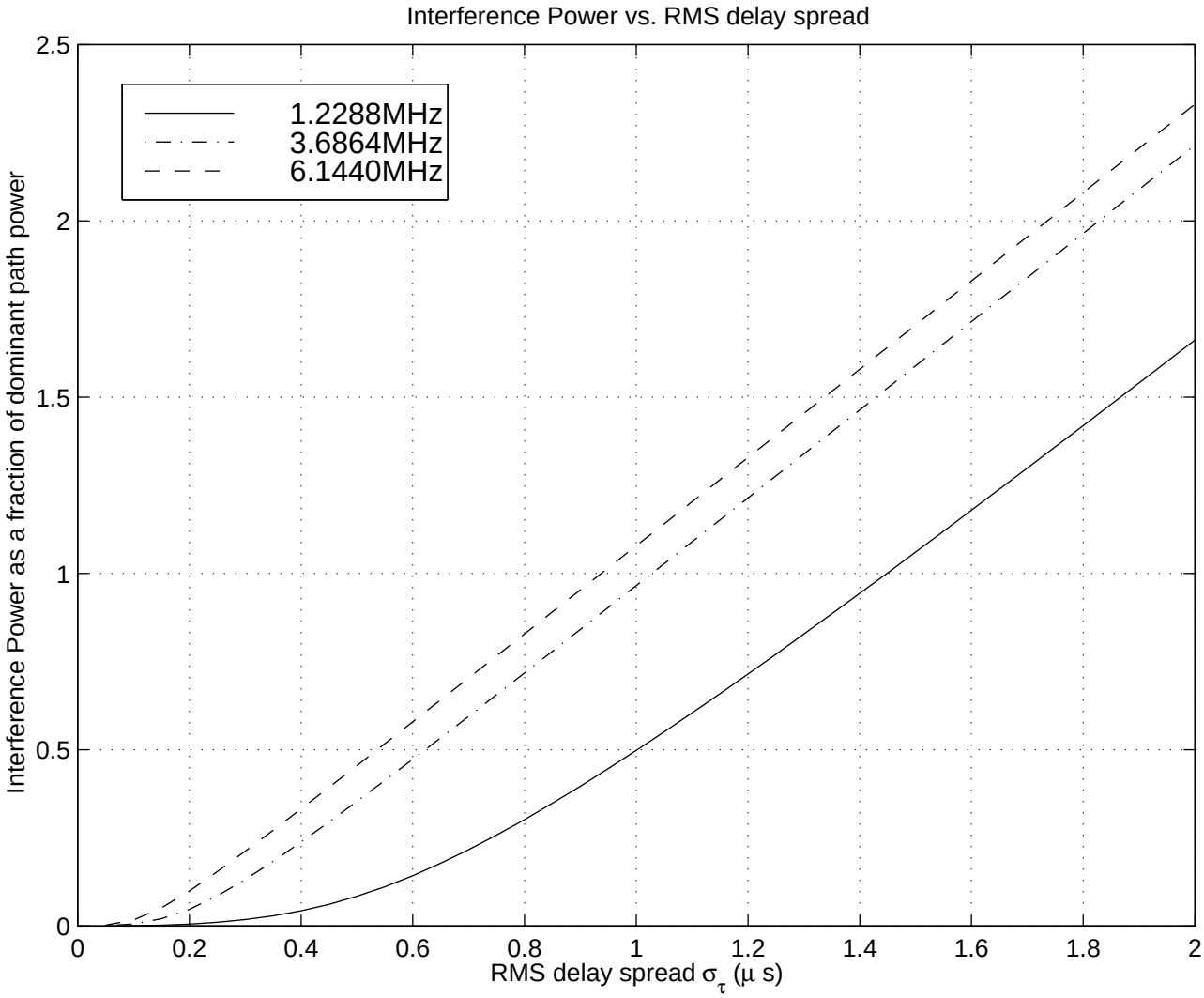

Figure 3.2: Intra-cell interference power as a function of RMS delay for three chip rates.

of orthogonal codes can reduce the local scattering interference to nearly zero if the RMS delay is small (less than $0.5\mu s$). As the RMS delay, σ_τ increases, the intra cell interference increases.

The RMS delay parameter is different for various environments and frequencies. In [35], for 910MHz in urban areas, the RMS delay spread, σ_τ, has an average value of $1.3\mu s$, and typically, the RMS delay spread increases for higher frequencies. Assuming the same value of $1.3\mu s$ in our simulations and analysis, this will yield an intra-cell interference power of approximately 0.7 to 1.4 times the direct path power (for chip rates of 1.2288MHz to 6.1140MHz).

These results on the effect of local scattering on intracell interference will be used throughout the analysis of downlink performance. We note that the inclusion of intracell interference increases the accuracy of our results.

3.4.3 Recursive Estimator using Kalman Filter

Assuming that the channel response vector (CRV) is approximately constant over a sufficiently short period of time, we can formulate the CRV estimation problem recursively using a Kalman filter. First, we observe that Equation (3.10) corresponds to the output equation for the Kalman filter. The constant CRV assumption is valid when the chip rate is very high compared to the fading rate. For a cell with N users and M antenna elements at the base station, the state and output equations for user

k, at time n, are, respectively,

$$\mathbf{a}_k(n+1) = \mathbf{F}(n)\mathbf{a}_k(n) + \mathbf{G}(n)\mathbf{U}(n) \tag{3.27}$$

$$y_k(n) = \mathbf{h}(n)\mathbf{a}_k(n) + V_k(n) \tag{3.28}$$

where

$$\mathbf{F}(n) = \mathbf{I}_{N\times N} \tag{3.29}$$

$$\mathbf{U}(n) \sim N(0, \sigma_D^2 \mathbf{I}_{N\times N}) \tag{3.30}$$

$$\mathbf{G}(n) = \mathbf{I}_{N\times N} \tag{3.31}$$

$$\mathbf{h}(n) = \mathbf{x}^T(n) \tag{3.32}$$

$$V(n) \sim N(0, Var\{I_k\} + \sigma_t^2) \tag{3.33}$$

where $\mathbf{I}_{N\times N}$ is the identity matrix of size $N \times N$ and σ_t^2 is the additive thermal noise power, σ_D^2 represent changes in the CRV $\mathbf{a}_k$ between samples due to a changes in mobile position. The notation $N(\mu, \sigma^2)$ represents a normal distribution with mean μ and variance σ^2. The quantity $\mathbf{h}(n)$ is a row vector. In (3.27), It is assumed the temporal changes in the CRV are completely random and independent of the CRV itself. The change is modeled as an additive white gaussian noise with variance σ_D^2. Interference noise is modeled as a Gaussian-distributed random variable with zero mean and variance I_k. The goal is to estimate the state $\mathbf{a}_k$ of the above discrete-time linear dynamic system for each user.

If the received signal $y_k(n)$ is fed back to the base station, the base station can use $y_k(n)$ together with the knowledge of the transmitted signal to estimate the CRV $\mathbf{a}_k$ for the k^{th} user without the need for any additional processing at the mobile.

The solution to the above standard state estimation problem is as follows, [32]:

$$\mathbf{a}_k(n) = \mathbf{a}_k(n-1) + \mathbf{K}(n)(y_k - \mathbf{h}(n)\mathbf{a}_k(n-1)) \tag{3.34}$$

where the gain matrix,

$$\mathbf{K}(n) = \mathbf{\Sigma}_{n|n-1}\mathbf{h}(n)^*[\mathbf{h}(n)\mathbf{\Sigma}_{n|n-1}\mathbf{h}(n)^* + Var\{I_i\} + \sigma_t^2]^{-1} \tag{3.35}$$

and state covariance matrix, $\mathbf{\Sigma}_{n|n-1}$, at time n given measurements is found using the recursions,

$$\mathbf{\Sigma}_{n|n} = \mathbf{\Sigma}_{n|n-1} - \mathbf{K}(n)\mathbf{h}(n)\mathbf{\Sigma}_{n|n-1} \tag{3.36}$$

$$\mathbf{\Sigma}_{n|n-1} = \mathbf{\Sigma}_{n-1|n-1} + \sigma_D^2 I_{N\times N} \tag{3.37}$$

Using the (3.34)-(3.37), we can estimate the CRV recursively. The dynamical model above accommodates slow changes in the CRV, which would arise in time-varying mobile channel.

An important advantage in implementing the CRV estimator using the above algorithm is its efficient use of computational resources. As each new sample is received, the innovations information present in the new sample is used to generate a better estimate of the CRV. The measurement at time n can be written as the estimate of the measurement based on previous observations plus some new information term, ι_n,

$$y_k(n) = \hat{y}_{k|k-1}(n) + \iota_n \tag{3.38}$$

It can be shown [32], the new information, ι_n in each new measurement is independent of the previous samples. In the implementation of the algorithm, the base station

requires memory to track the transmitted signal trajectory. Since only one vector needs to be stored for each time period, this memory requirement is low. This savings can be significant considering that a separate CRV estimator is required for each mobile in the cell.

3.4.4 Batch Processing using a Least-Squares Method

We can alternatively solve for the CRV by stacking L scalar measurements of the received signal for a particular user i at time n, $y_i(n)$, to form a matrix-vector equation. The transmitted base station signal vector at time n is $\mathbf{x}^T(n)$,

$$\mathbf{Y}_i(n) = \begin{bmatrix} y_i(n+1-L) \\ y_i(n+2-L) \\ \vdots \\ y_i(n) \end{bmatrix} \tag{3.39}$$

$$= \mathbf{X}(n)\mathbf{a}_i + \mathbf{N_i} \tag{3.40}$$

$$= \begin{bmatrix} \mathbf{x}^T(n+1-L) \\ \mathbf{x}^T(n+2-L) \\ \vdots \\ \mathbf{x}^T(n) \end{bmatrix} \mathbf{a}_i + \begin{bmatrix} \eta_i(n+1-L) \\ \eta_i(n-L) \\ \vdots \\ \eta_i(n) \end{bmatrix} \tag{3.41}$$

where the $\eta_i(n)$ is the measurement noise for the measurement at time n, and $\mathbf{x}^T(n)$ is a $M \times 1$ vector of transmitted signals from the base station with M antenna elements. For the downlink, the transmitted signal from the base station, $\mathbf{x}^T(n)$, is common to all users.

The CRV can be estimated by solving the above equation for $\mathbf{a}_i$. In order to solve for the CRV, the matrix $\mathbf{X}(n)$ must be of full column rank. A necessary condition is that L must be greater than or equal to the number of antennas M. In practice, to obtain an accurate estimate of $\mathbf{a}_i$ (with the associated desirable asymptotic properties when L is large), L must be significantly larger than M.

For the full rank case, the least-squares solution for $\mathbf{a}_i$ in (3.41) is well known. The estimated CRV at time n for the i^{th} user is,

$$\hat{\mathbf{a}}_i(n) = (\mathbf{X}(n)^T\mathbf{X}(n))^{-1}\mathbf{X}(n)^T\mathbf{Y}_i(n) \tag{3.42}$$

Computationally, the recursive estimator using the Kalman filter is more efficient, [32]. The increased computational complexity would make real-time implementation of batch processing more difficult. Another disadvantage of this batch processing method is that the model does not take into account changes in the CRV between the samples. Therefore, the estimate does not track changes in the CRV if it is changing slowly. Therefore, estimators based on a dynamical model, such as introduced in subsection 3.4.3, would be more desirable in situations where CRV may be changing slowly.

3.5 Power Assignment

In the previous section, a channel model was developed for the downlink channel. A channel estimator was also proposed based on the Kalman filter. The knowledge

of CRV for each user at the base station allows the base station to exploit spatial diversity to achieve a significant increase in SNR performance.

In this section, a power assignment algorithm based on [51] is extended to allow for multiple qualities of services (QoS). Using the power assignment algorithm combined with standard maximum SNR beamforming practices, a gain in SNR performance can be achieved.

Assuming we have a set of normalized beamforming weights, $\mathbf{v}_j$, for user j in the cell for all $1 \leq j \leq N$, we can assign a power level to each user such that the signal-to-interference plus noise ratio (SINR) at each user is the same as when there is no inter-cell interference. It has been proven that the SINR should be equalized for all users in the cell is to maximize the minimum SINR [51]. Intuitively, if the SINRs are not equal for all users, there would exist at least one user with a higher SINR than the user with the lowest SINR. The power to the user with higher SINR can therefore be reduced for the user with higher SINR, thereby decreasing the interference for other users, thereby raising the minimum SINR for the cell.

For the base station, we assume that only the CRVs from users within the cell are known. Therefore, we will solve the problem of maximizing minimum SINR for the single-cell situation, and later apply the result to the realistic situation of multiple cells.

For practical systems applications, the total power transmitted by the base station is limited. Therefore, the formulation for the problem of maximizing the minimum

SINR can be formulated as the following optimization problem:

$$maximize \ \ SINR_0 \ \text{such that} \ \sum_{i=1}^{N} k_i^2 = P \tag{3.43}$$

where k_i^2 is the assigned power for user i. The power k_i^2 will be determined by an algorithm to allocate a portion of total base station power such that after path-loss α_i and directional gain of the antenna, the effective SINR will be optimized for the i^{th} user. In (3.43) $SINR_0$ is defined as,

$$SINR_0 = \frac{\|\mathbf{a}_i^T \mathbf{v}_i\|^2 k_i^2 R_i^{-1}}{\sum_{j=1, j\neq i}^{N} \|\mathbf{a}_i^T \mathbf{v}_j\|^2 k_j^2 + \sigma_t^2} \frac{R_0}{W} \tag{3.44}$$

where R_i is the relative quality of service (QoS) for mobile user i, and R_0 is the base quality of service level. Vector $\mathbf{a}_i$ denotes the CRV for the path from the base station to mobile i. Here, we have taken into account the situation where different services share the same frequency band and time slots. A quality of service is achieved by weighing each user's SINR.

To ensure a certain level of service, the SINR at a particular mobile site must be above a certain level threshold for that service. In environments where several different levels of services are available, the desired SNR level for each service may be a multiple of some base level of service. To provide for different service, a different SINR is necessary for each service. Services that require higher SINR, therefore will be provided with more power.

The solution to the above problem is solved by [51] for the case where all users have the same service. To solve this with different levels of services available, we generalize the procedure outlined in [51].

From equations (3.43) and (3.44), we generalize [51] for multiple rates of service as follows: first we rearrange the (3.44) as follows:

$$\frac{k_i^2}{R_i} = SINR_0 \frac{W}{R_0} \sum_{j=1, j\neq i}^{N} \frac{\|\mathbf{a}_i^T \mathbf{v}_j\|^2 k_j^2}{\|\mathbf{a}_i^T v_i\|^2} + \frac{\sigma^2}{\|\mathbf{a}_i^T \mathbf{v}_i\|^2} \tag{3.45}$$

$$= SINR_0 \frac{W}{R_0} R_i \mathbf{g}(i)^T \mathbf{k} + \varrho \tag{3.46}$$

where $\mathbf{g}(i)$ is an N-element vector of normalized dot (scalar) products between the vectors $\mathbf{a}_i$ and $\mathbf{v}_j$. Vector $\mathbf{k}$ is a column vector with elements k_i.

$$g(i)_j = \begin{cases} \frac{\|\mathbf{a}_i^T \mathbf{v}_j\|^2}{\|\mathbf{a}_i^T \mathbf{v}_i\|^2} & j = 1 \ldots N, i \neq j \\ 0 & i = j \end{cases} \tag{3.47}$$

$$\mathbf{g}(i) = [g(i)_1, g(i)_2, \cdots, g(i)_N]^T \tag{3.48}$$

$$\mathbf{k} = [k_1, k_2, \ldots, k_N]^T \tag{3.49}$$

$$\varrho = \left[\frac{\sigma^2}{\|\mathbf{a}_1^T \mathbf{v}_1\|^2}, \cdots \frac{\sigma^2}{\|\mathbf{a}_N^T \mathbf{v}_N\|^2} \right] \tag{3.50}$$

where $g(i)_j$ denotes the j^{th} element of the vector $\mathbf{g}(i)$.

At this point, we define a vector denoting the known target QoS for each user is as,

$$\mathbf{s} = [R_1, R_2, \ldots, R_N]^T \tag{3.51}$$

We express the equations (3.43) and (3.46) in matrix form, as:

$$\mathbf{Cy} = SINR_0 \mathbf{By} \tag{3.52}$$

$$\mathbf{Dy} = \mathbf{C^{-1}By} = \frac{1}{SINR_0} \mathbf{y} \tag{3.53}$$

where,

$$\mathbf{y} = [\mathbf{k} \;\; 1] \tag{3.54}$$

$$\varsigma = [R_1^{-1} \;\; R_2^{-1} \;\; \ldots \;\; R_N^{-1}] \tag{3.55}$$

$$\mathbf{S} = \begin{bmatrix} R_1 & & \\ & \ddots & \mathbf{0} \\ \mathbf{0} & & \\ & & R_N \end{bmatrix} \tag{3.56}$$

$$\mathbf{C} = \begin{bmatrix} \mathbf{S^{-1}} & 0_{N\times 1} \\ \mathbf{1}_{1\times N} & -P \end{bmatrix} \tag{3.57}$$

$$\mathbf{1}_{1\times N} = [\overbrace{1, 1, \cdots, 1}^{N}] \tag{3.58}$$

$$\mathbf{G} = \begin{bmatrix} \mathbf{g}(1) \\ \mathbf{g}(2) \\ \vdots \\ \mathbf{g}(N) \end{bmatrix} \tag{3.59}$$

$$\mathbf{B} = \begin{bmatrix} \mathbf{G} & \varrho \\ 0_{1\times N} & 0 \end{bmatrix} \tag{3.60}$$

$$\mathbf{D} = \begin{bmatrix} \mathbf{SG} & \mathbf{s}^T\varrho \\ (\varsigma^T)\mathbf{G} & \varrho^T\mathbf{s}/P \end{bmatrix} \tag{3.61}$$

In (3.57) and (3.61), P is defined as in (3.43) as the total power available to the base station transmitter.

The solution to maximizing the minimum SINR is the eigenvector of $\mathbf{D}$ in (3.53) corresponding to the largest eigenvalue. The eigenvector of $\mathbf{D}$ must be scaled so

that the last element is one. The largest eigenvalue will be the inverse of the lowest achievable SINR. It was proven by Yang and Xu in [51] that the largest eigenvalue is positive, and the elements of the scaled eigenvector are all non-negative. We have verified the proof given in [51].

3.6 Directional Beamforming Vector for the Downlink Channel

To apply the power allocation algorithm described in the previous section, we must determine a set of directional beamforming weight vectors. There are two obvious candidate methods to estimate a set of directional beamforming weight vectors. First, we can use the conjugate of the CRV corresponding to the desired user corresponding to maximum SNR beamforming (or max-SNR) [30]. Alternatively, we could use a form of Capon's Minimum Variance Estimator (MV), also known as the maximum SINR beamforming (max-SINR) [30].

Maximum SNR beamforming maximizes the energy transmitted to the desired user, for a fixed transmission power. For maximum SINR beamforming, the energy transmitted to the desired user is maximized while intra-cell interference energy is minimized. The intra-cell SINR in a multi-user environment ignoring inter-cell interference can be expressed as,

$$SINR_{intracell} = \frac{\|\mathbf{w}_i^* \mathbf{a}_i\|}{\mathbf{w}_i^* \sum_{\substack{k=1 \\ k \neq i}}^{N} \mathbf{a}_k \mathbf{a}_k^* \mathbf{w}_i + \sigma_t^2} \tag{3.62}$$

where σ_t is the variance of the thermal noise.

Assuming the system is interference limited, to maximize SINR, we are seeking to minimize the total received power while holding the desired user's power constant. The max-SINR beamformer for the i^{th} user, $\mathbf{w}_i$ can be formulated as follows,

$$\underset{\mathbf{w}_i}{minimize} \quad \mathbf{w}_i^* \sum_{k=1}^{N} \mathbf{a}_k \mathbf{a}_k^* \mathbf{w}_i \;\; such\ that \;\; \|\mathbf{w}_i^* \mathbf{a}_i\| = 1 \tag{3.63}$$

The solution, $\mathbf{w}_i$, is given in [6],

$$\mathbf{w}_i = \frac{\left(\sum_{k=1}^{N} \mathbf{a}_k \mathbf{a}_k^*\right)^{-1} \mathbf{a}_i}{\mathbf{a}_i^* \left(\sum_{k=1}^{N} \mathbf{a}_k \mathbf{a}_k^*\right)^{-1} \mathbf{a}_i} \tag{3.64}$$

If the number of users is less than the number of antenna elements, $\sum_{k=1}^{N} \mathbf{a}_k \mathbf{a}_k^*$ can be ill-conditioned. When the term is ill-conditioned, a psuedo-inverse operation must be performed in place of the inverse operation.

3.7 Algorithm Summary

In this chapter, a three-part algorithm was presented to perform the CRV-based power control for the downlink with multiple antenna elements at the base station. The steps in the algorithm are summarized in this section.

First, the base station stores the transmitted signal $\mathbf{x}(n)$ at time n. The k^{th} user feeds the received scalar signal, $y_k(n)$, back to the mobile. At the base station, the CRV, $\mathbf{a}_k(n)$, is estimated using a Kalman filter based algorithm from the fed-back signal and stored transmitted signal. The recursions are,

$$\mathbf{a}_k(n) \;\; = \;\; \mathbf{a}_k(n-1) + \mathbf{K}(n)(y_k - \mathbf{h}(n)\mathbf{a}_k(n-1)) \tag{3.65}$$

$$\mathbf{K}(n) = \mathbf{\Sigma}_{n|n-1}\mathbf{h}(n)^*[\mathbf{h}(n)\mathbf{\Sigma}_{n|n-1}\mathbf{h}(n)^* + Var\{I_i\} + \sigma_t^2]^{-1} \tag{3.66}$$

the state covariance matrix, $\Sigma_{n|n-1}$, are given as,

$$\mathbf{\Sigma}_{n|n} = \mathbf{\Sigma}_{n|n-1} - \mathbf{K}(n)\mathbf{h}(n)\mathbf{\Sigma}_{n|n-1} \tag{3.67}$$

$$\mathbf{\Sigma}_{n|n-1} = \mathbf{\Sigma}_{n-1|n-1} + \sigma_D^2 I_{N\times N} \tag{3.68}$$

With the knowledge of the CRV for all N users, $\mathbf{a}_i$ $(1 \leq i \leq N)$ we can find a directional beamforming weight vector for each user i, $\mathbf{w}_i$. Two methods were proposed for finding a suitable directional beamforming weight vector. For user i, we can either use its CRV, $\mathbf{a}_i$, as the beamforming weight vector,

$$\mathbf{w}_i = \mathbf{a}_i \tag{3.69}$$

Alternatively, we can the use maximum SINR method,

$$\mathbf{w}_i = (\sum_{k=1}^{N} \mathbf{a}_k\mathbf{a}_k^*)^{-1}\mathbf{a}_i \tag{3.70}$$

Once we have the directional beamforming weight vectors, we can normalize them,

$$\mathbf{v}_i = \frac{\mathbf{w}_i}{\|\mathbf{w}_i\|^2} \tag{3.71}$$

Then, we can find the power allocation for each user that will result in the maximize the minimum guaranteed SINR by finding the eigenvector of $\mathbf{D}$ corresponding to the largest eigenvalue. The $(N+1)\times(N+1)$ matrix $\mathbf{D}$ is defined as,

$$\mathbf{D} = \begin{bmatrix} \mathbf{SG} & \mathbf{s}^T\varrho \\ (\varsigma^T)\mathbf{G} & \varrho^T\mathbf{s}/P \end{bmatrix} \tag{3.72}$$

where

$$\mathbf{S} = \begin{bmatrix} R_1 & & \\ & \ddots & \mathbf{0} \\ \mathbf{0} & & \\ & & R_N \end{bmatrix} \tag{3.73}$$

$$\mathbf{G} = \begin{bmatrix} \mathbf{g}(1) \\ \mathbf{g}(2) \\ \vdots \\ \mathbf{g}(N) \end{bmatrix} \tag{3.74}$$

$$\mathbf{1}_{1\times N} = [\overbrace{1, 1, \cdots, 1}^{N}] \tag{3.75}$$

$$\mathbf{s} = [R_1, R_2, \ldots, R_N]^T \tag{3.76}$$

$$\mathbf{g}(i) = [g(i)_1, g(i)_2, \cdots, g(i)_N]^T \tag{3.77}$$

$$\varrho = \left[\frac{\sigma^2}{\|\mathbf{a}_1^T\mathbf{v}_1\|^2}, \cdots \frac{\sigma^2}{\|\mathbf{a}_N^T\mathbf{v}_N\|^2}\right] \tag{3.78}$$

$$g(i)_j = \begin{cases} \frac{\|\mathbf{a}_i^T\mathbf{b}_j\|^2}{\|\mathbf{a}_i^T\mathbf{b}_i\|^2} & j = 1\ldots N, i \neq j \\ 0 & i = j \end{cases} \tag{3.79}$$

The eigenvector of $\mathbf{D}$ which corresponds to the largest eigenvalue is a $N+1$ element vector. If the last element of the eigenvector is normalized to one, then the first N elements will correspond to the power allocation for each user i ($1 \leq i \leq N$).

3.8 Summary

In this chapter, a model of the downlink synchronous CDMA channel is presented. In this model, we take into account the following effects:

- Effects of path-loss and shadowing.
- Multi-cell interference caused by asynchronous reception from base stations for adjacent cells.
- Intra-cell interference caused by delay spread within the cell resulting in asynchronous reception of multipath signals.

A algorithm is presented to perform downlink beamforming in three steps:

1) Channel estimation using feedback from each user with no pilot signal

2) Generation of directional beamforming weights for each user

3) Jointly allocate Power to each user to maximize the minimum guaranteed SINR

To estimate the CRV for a dynamic channel, a recursive and a batch processing algorithms are presented. Using the CRV from the channel estimator, a beamforming algorithm is presented using the CRV for generating directional beamforming weights. A power allocation algorithm is presented for allocating power to each user. The algorithm allows the base station to perform downlink beamforming with minimal computational resources at the mobile station. With downlink beamforming, the base station can utilize spatial diversity to improve the SNR for each user.

Chapter 4

Numerical and Simulation Results on CDMA downlink

4.1 Introduction

There have been previous studies on optimizing the beamforming weights for base station antenna arrays in the uplink on per-user basis, such as by Naguib, Paulraj and Kailath in [23] [24], but there have been considerably fewer studies on the improvements due beamforming and power allocation for the downlink channel. In CDMA, the cell base station broadcasts information to all mobiles at the same time. Assuming that the mobiles are all far enough away from the array and there is negligible scattering, the signal wavefront is approximately planar. With an antenna array, by adjusting the phase of the each antenna element carefully, we can ensure that the

desired user will receive the signal coherently at the direction of desired mobile location, and incoherently elsewhere. The antenna gain at each spatial location is a function of the angle between mobile and base station and the beamforming weights. Therefore, spatial diversity allows the base station to transmit signals weighted in such a manner to minimize the signal gain over most angles while maximizing the signal in the desired direction.

In this chapter, performance of the CRV-based power control algorithm presented in Chapter 3 is studied through numerical methods and simulation. First, the performance of the recursive CRV estimator is studied through both simulation and a simplified analysis in a multi-cell, multi-user environment as a function of the number of antenna elements at the base station.

Also, the uncoded SINR performance is studied using Monte Carlo integration [28], with inter-cell interference in a synchronous CDMA system. The uncoded SINR is calculated as the ratio of signal power divided by total interference and noise power. The performance is evaluated for a multi-cell, multi-user environment. In each Monte Carlo integration, 500 different scenarios are generated.

For Monte Carlo integration [28], the path-loss and shadowing coefficients are 4 and 8 dB, respectively as presented earlier in section 3.4.2.

In our simulations, we assume we have a direct or dominant path. The multipath components of the signal are due to local scattering along the direct or dominant path. The resulting intra-cell interference is 0.3 times the direct path power, corresponding

to a 0.8 μs RMS delay spread.

To simulate a realistic mobile environment, interfering base stations are present surrounding the central cell in two tiers, [14]. Each interfering cell contains the same number of mobiles as the center cell, and employs the same beamforming algorithm. The results are presented for 3 to 33 continuously transmitting users per cell. The users are uniformly distributed in the cell, and there CRV is assumed to be constant.

4.2 Performance of the Kalman Filter

Since the dynamical model of the CRV as given in Equations (3.27) (3.28) is linear, time-invariant, and asymptotically stable, the state estimate approaches a steady state value. Since the Kalman filter approaches a steady state, the estimation error should approach $\Sigma_{\infty|\infty}$ [32]. The steady state covariance matrix can be calculated in closed-form for the case of a single antenna, but the expression is more complicated as the number of antenna elements increases. For scenarios where the number of antenna elements is greater than one, the measurement update equation (3.36) becomes a discrete-time Riccati equation as n goes to infinity. The steady state covariance matrix can be solved using numerical solutions to the discrete-time Riccati equation.

For the single antenna case, the theoretical steady state error for the CRV (which contains only the attenuation experienced for a particular user) is the same as the scalar version of the Kalman filter minimum mean squared error (MMSE) which can

be calculated as [32]:

$$MMSE_{theoretical}(CRV) = \frac{1}{2}(\sigma_D^4 + 4\sigma_D^2(E\{I_i\} + \sigma_t^2))^{1/2} + \sigma_D^2 \tag{4.1}$$

I_i is defined in (3.3). For one antenna, the base station signal is omni-directional, i.e., $G_i(r,\theta) = 1$. We repeat (3.3) below for future reference.

$$I_i = \| \sum_{l=2}^{l=L} \mathbf{a}_{i,l,1}^* \mathbf{x}_1(t - \tau_{i,l,1}) + \sum_{k=2}^{k=K} \sum_{l=1}^{l=L} \mathbf{a}_{i,l,k}^* \mathbf{x}_k(t - \tau_{i,l,k}) \|^2 \tag{4.2}$$

To find the average interference from other base stations, we assume that the total power transmitted for each base station is the same. The attenuation experienced by the signal from the i^{th} base station can be evaluated using (3.22), which is repeated below:

$$E\{PL_i\} = e^{\frac{\sigma_S^2}{200} log(10)^2} \int_0^{2\pi} \int_0^R G_i(r,\theta) \frac{r}{(r^2 + B_i^2 - 2B_i r cos(\theta - \vartheta))^2} d\theta dr \tag{4.3}$$

If there is more than one antenna at the base station, the actual calculation of I_i in (4.2) becomes difficult. If we assume that no beamforming is performed at the base station, and the interference power is dependent only on the distance between mobile and interfering base stations only, we can find the steady state error for the estimator. The steady state error variance, $\Sigma_{\infty|\infty}$ can be calculated as the solution of the following discrete time algebraic Riccati equation [3]:

$$\begin{aligned} \Sigma_{\infty|\infty} \quad = \quad & \Sigma_{\infty|\infty}\sigma_D^2 \mathbf{I}_{N\times N} - (\Sigma_{\infty|\infty} + \sigma_D^2 \mathbf{I}_{N\times N})\mathbf{H}^*(n) \\ & [\mathbf{H}(n)(\Sigma_{\infty|\infty} + \sigma_D^2 \mathbf{I}_{N\times N})\mathbf{H}^*(n) + I_t + \sigma_t^2]^{-1} \\ & \mathbf{H}(n)(\Sigma_{\infty|\infty} + \sigma_D^2 \mathbf{I}_{N\times N}) \end{aligned} \tag{4.4}$$

The above equation can be used to quantify the effect of increasing the number of antenna elements in the antenna array on the steady state estimation error. We can solve (4.4) numerically, and express the result as a percentage of the expected magnitude of the CRV, if σ_D^2 is given. In the following, we will calculate the MMSE for several different values of σ_D^2

For the variance of the CRV, σ_D^2, of 0.01% of the magnitude of the CRV per sample, we obtain Table 4.1.

Number of Elements	$MMSE_{theoretical}$
1	0.0011%
3	0.0110%
5	0.0211%
7	0.0311%

Table 4.1: Theoretical Steady State Variance for estimating CRV (with CRV changing with a variance of 0.01% of the norm of the CRV from one sample to the next) .

For larger values, e.g. for σ_D^2 equal to 1% of the norm of the CRV, the theoretical values are shown in Table 4.2.

By increasing the number of elements in the array, the thermal noise is increased. Therefore, degradation in the steady state variance of the estimator should be expected.

Number of Elements	$MMSE_{theoretical}$
1	1.59%
3	2.38%
5	3.04%
7	4.22%

Table 4.2: Theoretical Steady State Variance for estimating CRV (with CRV changing with variance of 1% of the norm of the CRV from one sample to the next) .

To test the performance of the Kalman filter, simulations were performed in an environment with 20 continuously transmitting users per base station and 18 interfering base stations. We consider the performance in a generic synchronous CDMA system. For the purpose of the simulation, we assume that no multipath exists. Twenty mobiles are placed randomly (spatially uniformly distributed) in the center cell. The normalized CRV for each mobile in the center cell is generated using the ideal array response for a circular array with inter-element spacing of half a wavelength plus a normally distributed random variable with zero mean and the variance equal to ten percent of the magnitude of the CRV. The antenna elements are assumed to be within the same plane as the mobiles, i.e. zero elevations is assumed. The magnitude of CRV is determined by multiplying the normalized CRV by the path-loss factor, with ξ equal to 4, and shadowing variance σ_S^2 equal to 8 dB. In our simulations, we assume the feedback is achieved through a separate channel, and in the scope of this chapter, we assume an error-free feedback channel. The received amplitude at the mobile is fed

back to the base station during the next sample period, and the estimated CRV is updated. The feedback delay in the system is one sample. Therefore, each sample period corresponds to the feedback period. Beamforming is performed digitally at the base station using a maximum SNR beamforming method as presented in Section 3.6.

The estimation error of the Kalman filter as a function of number of feedback samples received, assuming the CRV experiences no drift, are shown in Fig. 4.1.

From Fig. 4.1, several observations can be made. The estimation error for a particular number of samples received increases as the number of antenna elements is increased. One explanation for higher estimation error when using more antenna elements may be due to the fact that more parameters are estimated. Therefore more data samples are needed to estimate the parameters to the same degree of accuracy. Since the CRV for each user is not changing between samples ($\sigma_D^2 = 0$), the steady state MMSE goes to zero as the number of samples goes to infinity.

In Fig. 4.2, we observe the scenario where the CRV is affected by an additive change modeled by a random variable with variance equal to 0.01% of the expected norm of the CRV between each sample. Since the CRV is changing between samples, the estimated CRV no long converge to the actual CRV. The observed steady state results from simulation are better than the theoretical values shown in Table 4.3. In the theoretical results, we assume that no beamforming is performed at interfering base stations so the state error can be solved by solving the corresponding digital

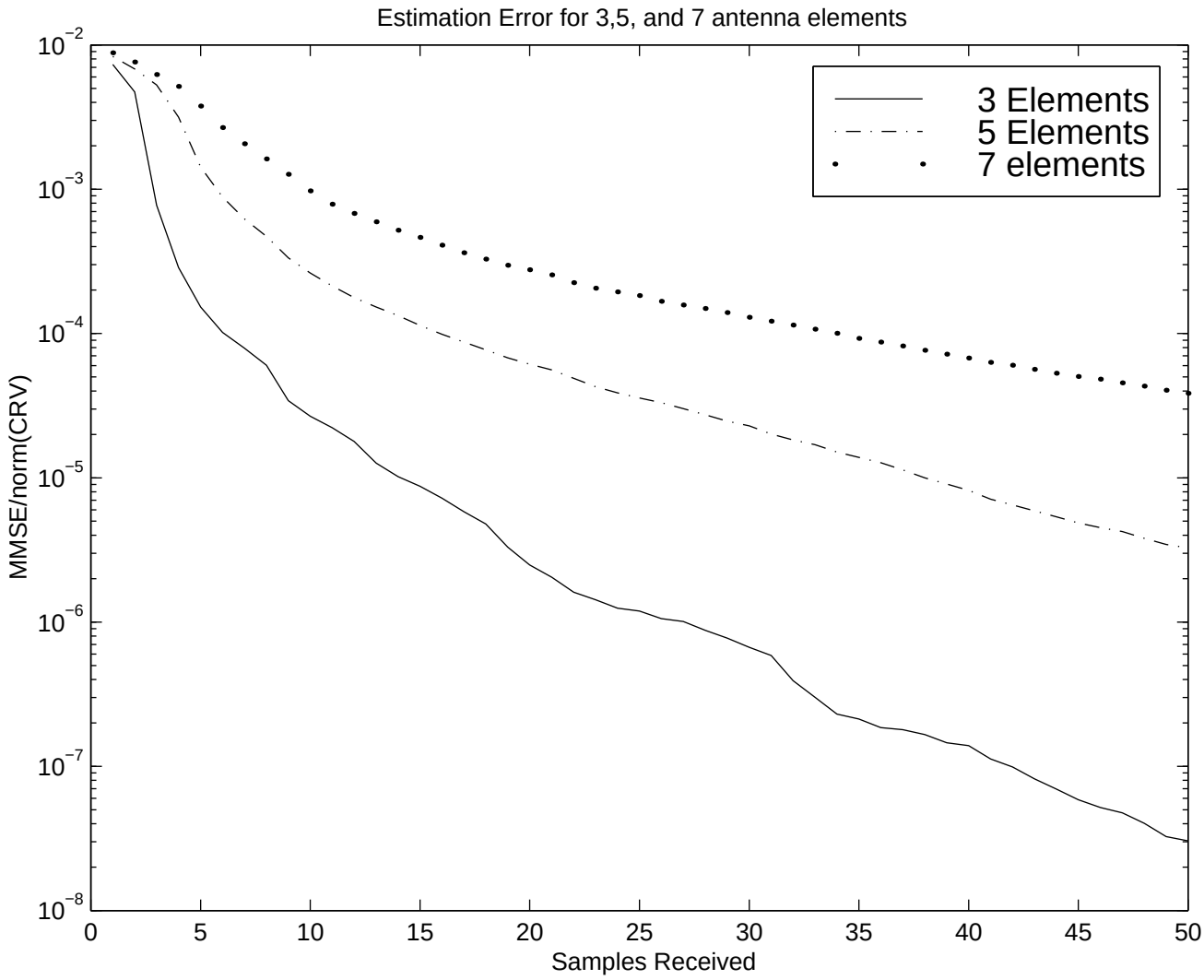

Figure 4.1: Estimation Error Using Kalman Filter with constant CRV.

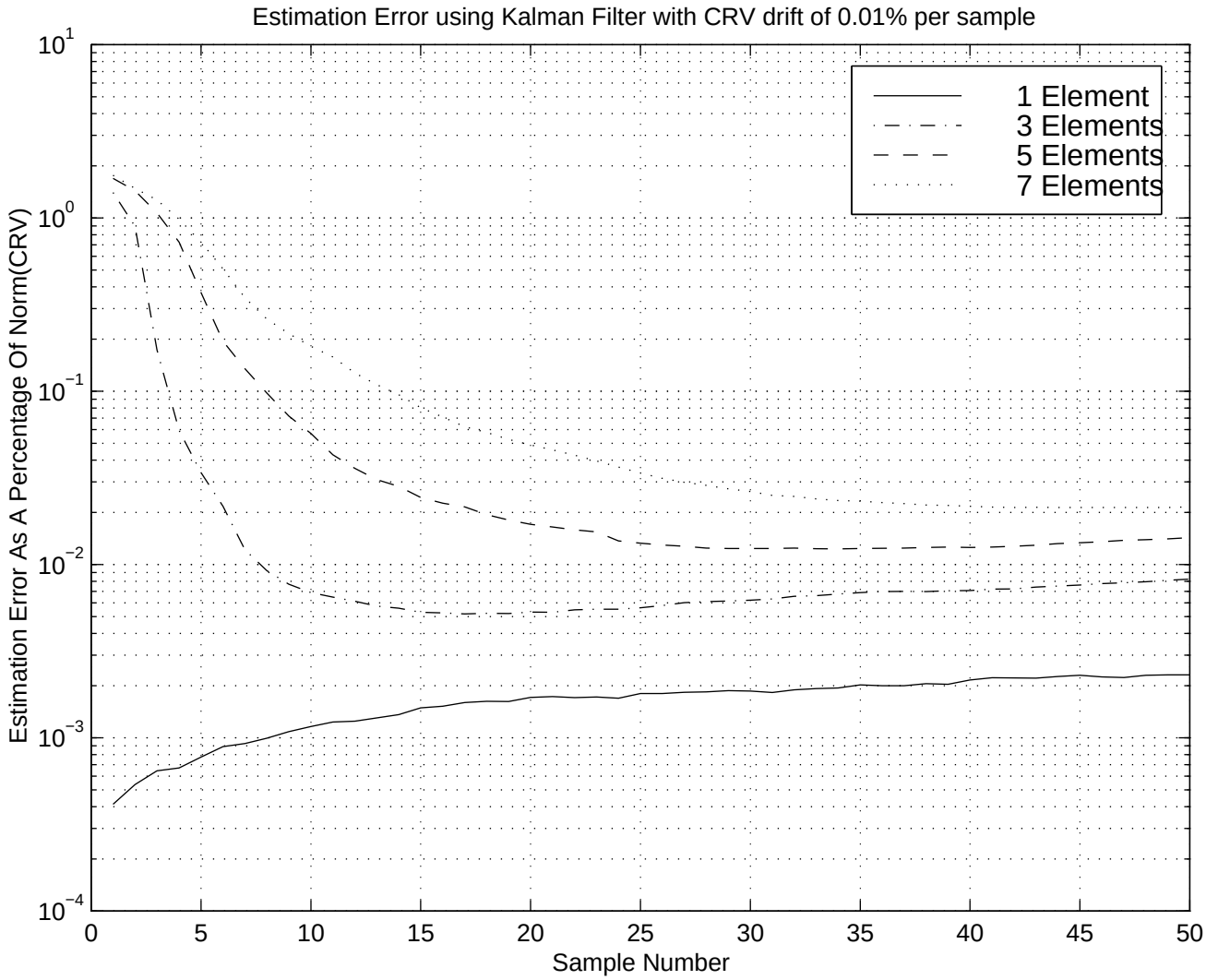

Figure 4.2: Estimation Error Using Kalman Filter with CRV experiencing a 0.01% drift per received sample.

Riccati equations. Since beamforming is performed at all interfering base stations, the inter-cell interference experience at the mobile will be less than if no beamforming is performed (as assumed in calculations $MMSE_{theoretical}$).

Number of Elements	$\text{MMSE}_{\text{theoretical}}$	Experimental
1	0.0011%	0.0012%
3	0.0110%	0.008%
5	0.0211%	0.015%
7	0.0311%	0.021%

Table 4.3: Comparison of analytical and simulated steady-state variance for estimating CRV (with σ_D^2 0.01% of the norm of the CRV) .

For a scenario where the CRV is changing significantly between samples, we model the change in CRV by an additive guassian distributed random variable with variance equal to 1% of the norm of the CRV. The theoretical and experimental results are shown in Table 4.4.

This section has illustrated the existence of an effective method for the estimation of CRV. The steady state estimation error for the estimator is shown to be small compared to the magnitude of the CRV.

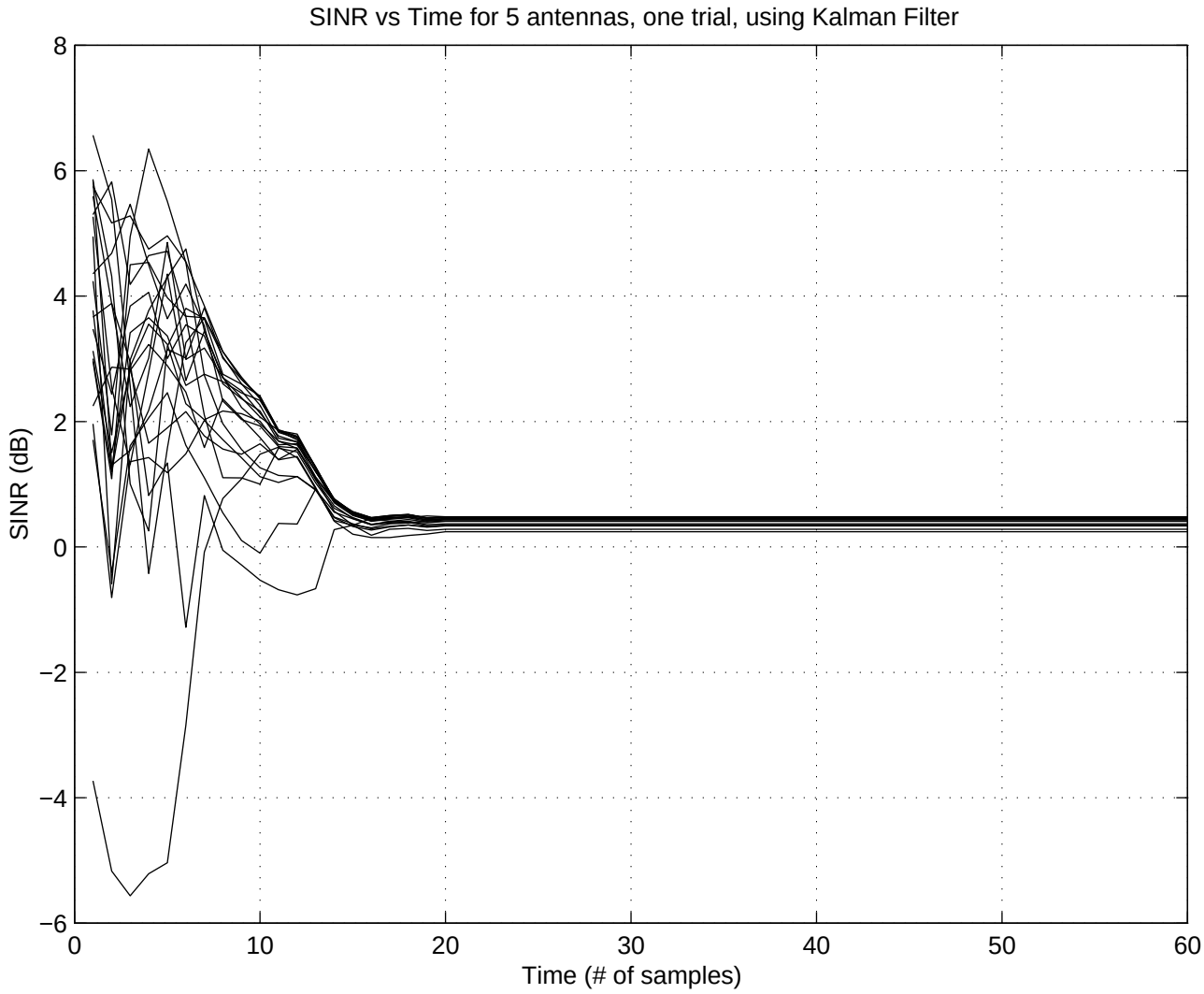

Figure 4.3: Sample paths of the SINRs for the 20 users in the cell are plotted. The minimum SINR improves over time as Kalman Filter reaches a steady-state.

Number of Elements	$\text{MMSE}_{\text{theoretical}}$	Experimental
1	1.59%	1.2928%
3	2.38%	2.0829%
5	3.04%	2.6132%
7	4.22%	3.6922%

Table 4.4: Comparison of analytical and simulated steady-state variance for estimating CRV (with σ_D^2 1% of the norm of the CRV).

4.3 Effect of CRV estimation error on Maximum SNR Beamforming

As can been seen from the results presented, small errors exist in the steady state for a Kalman filter based CRV estimator. The reason for the small amount of error at steady state is due to changes in CRV over time. In this section, we will study the effects of this steady state error on the SINR for base stations employing antenna arrays and beamforming.

For maximum-SNR beamforming, the weight vector used for beamforming is the complex conjugate of the CRV [30]. Without loss of generality, we can examine the effect of a small steady state error on the output of the beamformer for the i^{th} user.

We suppose that the CRV for the i^{th} user is $\mathbf{a}_i$, and that the beamforming weight

for the user is $\mathbf{w}_i$. The ideal output power should be:

$$|\mathbf{w}_i^T \mathbf{a}_i| = |\mathbf{a}_i^* \mathbf{a}_i| \tag{4.5}$$

If there is an error in the estimated CRV, $\hat{\mathbf{a}}_i$, then the beamform weight vector will be the complex conjugate of the estimated CRV instead of the complex conjugate of the actual CRV. The resulting output power would be:

$$|\mathbf{w}_i^T \mathbf{a}_i| = |\hat{\mathbf{a}}_i^* \mathbf{a}_i| \tag{4.6}$$

The Euclidean norm of the difference between using the perfect CRV and the CRV estimate is:

$$\begin{aligned} |\hat{\mathbf{a}}_i^* \mathbf{a}_i - \mathbf{a}_i^* \mathbf{a}_i| &= |(\hat{\mathbf{a}}_i^* - \mathbf{a}_i^*)\mathbf{a}_i| && (4.7) \\ &\leq \|\hat{\mathbf{a}}_i - \mathbf{a}_i\| \|\mathbf{a}_i\| && (4.8) \\ &= \epsilon_{CRV} \|\mathbf{a}_i\| \|\mathbf{a}_i\| && (4.9) \\ &= \epsilon_{CRV} \|\mathbf{a}_i\|^2 && (4.10) \end{aligned}$$

where ϵ_{CRV} is the relative error of the CRV estimate. In (4.8), we use the Schwarz inequality to bound the error. Therefore, the relative error between the ideal output power and the output power using an estimated CRV is bounded by the relative error of the CRV estimate. The maximum power loss is small if the error is small. The SINR loss due to maximum SNR beamforming using an estimated CRV can be quantified using values in Table 4.5 as:

For CRV changes of 1% between samples, the corresponding SINR loss is tabulated in 4.6 as,

Number of Elements	$\text{MMSE}_{\text{theoretical}}$	Experimental
1	-0.0048dB	-0.0052dB
3	-0.0480dB	-0.0349dB
5	-0.0922dB	-0.0656dB
7	-0.1372dB	-0.0922dB

Table 4.5: Theoretical and simulated steady-state power loss due to estimation error with CRV changing 0.01% between sample .

The use of maximum SINR beamforming method is much more difficult and beyond the scope of this thesis. However results presented in Sections 4.5 suggest that the use of maximum SNR beamforming method is superior to maximum SINR beamforming.

We conclude that the use of an estimated CRV as the basis for beamforming will result in a small loss compared to the use of the actual CRV for beamforming. In the next few sections, we will study the SINR performance of downlink beamforming in various multi-cell scenarios, assuming perfect CRV estimation.

4.4 Performance with Mixed Qualities of Service

The performance metric presented in the subsequent sections will be the uncoded SINR. The SINR after despreading will be multiplied by the processing gain [33]. In our study of multi-cell downlink performance, we assume a relative interference

Number of Elements	$\text{MMSE}_{\text{theoretical}}$	Experimental
1	-0.0696dB	-0.0565dB
3	-0.1046dB	-0.0914dB
5	-0.1341dB	-0.1150dB
7	-0.1873dB	-0.1634dB

Table 4.6: Theoretical and simulated steady-state power loss due to estimation error with CRV changing 1% between sample .

level due to delay spread of 0.3, corresponding to a delay spread of $0.8\mu s$ for a chip frequency of 1.2288MHz, or $0.4\mu s$ for chip frequency of 6.144MHz.

If there are several levels of service, the desired SINR levels would be higher for certain services than for others, and power allocation algorithms must provide more power to users using services requiring a higher quality of service.

To test the performance in an environment with two levels of service, i.e., where users have a choice of two levels of target SINR, the higher level service will be allocated twice as much power relative to the lower level of service. Therefore the QoS factor for the higher level of service is two, and the lower level of service has a factor of one. The resulting SINR is scaled by the level of service and plotted verses the percentage of users requiring the higher level of service.

In the simulations, the sum of the QoS factors for all mobiles remain constant. If a greater proportion of users use the higher level of service, the total number of users

decreases. The simulation results are shown in Fig. 4.4. The figure shows that the weighted SINR remains constant even though more users are using the higher quality service, as long as the overall SINR remains constant. The weighted SINR for user i using service R_1 as defined in (3.51) is calculated as in (4.11).

$$\text{Weighted SINR for user } i = \frac{SINR_i}{R_i} \tag{4.11}$$

The simulation results suggest, the overall weighted SINR will not degrade even if multiple levels of service is used.

4.5 Comparing Maximum SINR and Maximum SNR Beamforming Techniques

Assuming that mobiles are uniformly distributed within a cell, we can find the expected SINR performance by using Monte Carlo integration [28]. The expected SINR performance of maximum SINR and maximum SNR beamforming techniques are compared through the Monte Carlo integrator. The difference between maximum SINR and maximum SNR beamforming techniques in terms of SINR can be seen in Figure 4.5 and Figure 4.6 for the cases of three and five antenna elements, respectively.

For maximum SNR beamforming, no assumptions concerning spatial locations of interfering mobiles are made. In contrast, for maximum SINR beamforming, the spatial locations of intra-cell interferers are assumed known. However, we assume

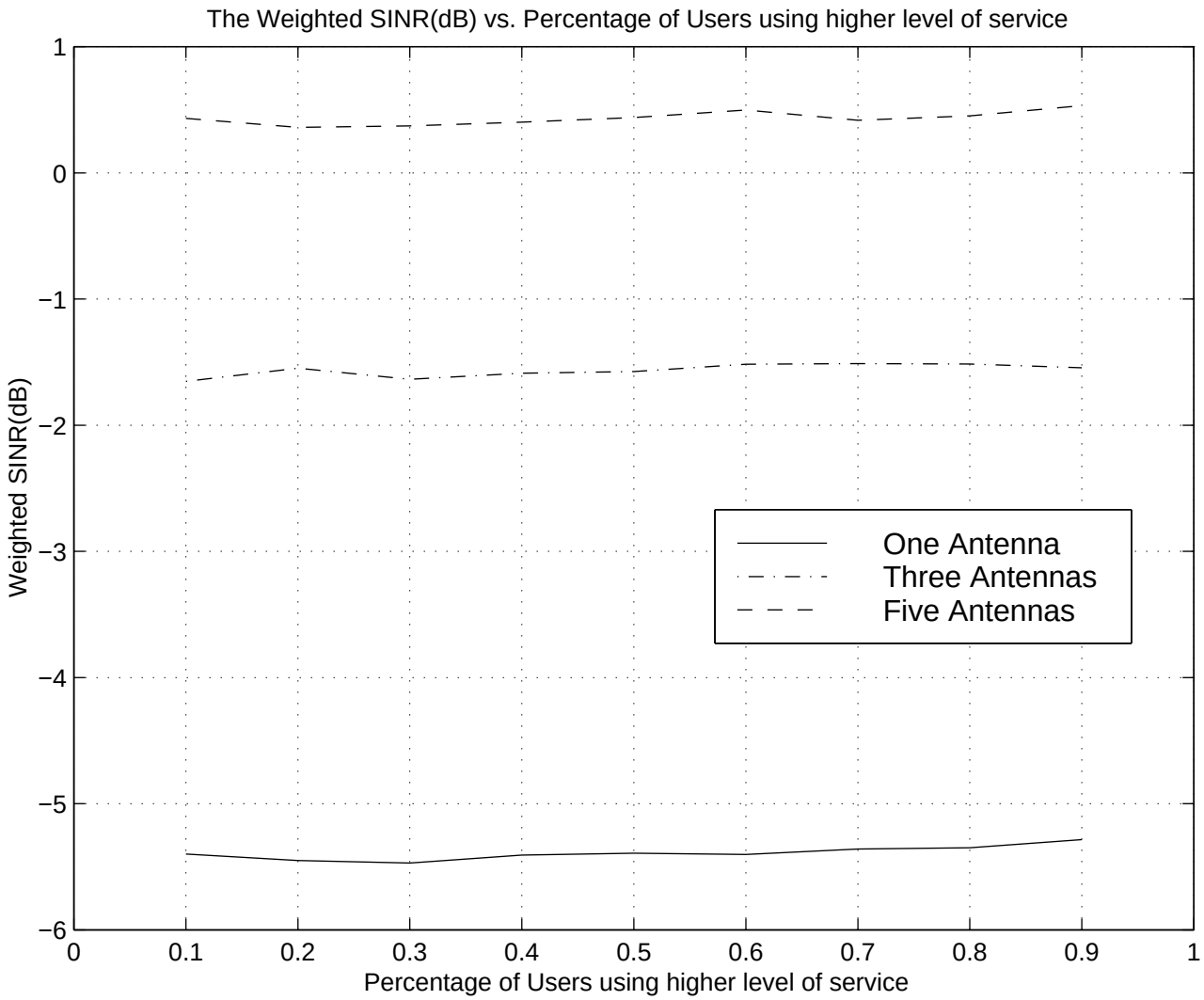

Figure 4.4: Performance as a function of the percentage of users using higher level of service.

that maximum SINR beamforming does not take into account interference that affects neighboring cells. For these definitions of maximum SNR and maximum SINR beamforming, the results (Figure 4.5 and Figure 4.6) show that maximum SNR beamforming outperforms maximum SINR beamforming. The result suggests that maximum SINR beamforming, which ignores intercell MAI, performs worse than maximum SNR beamforming when the number of users is greater than five. Theoretically, as the number of uniformly distributed users becomes very large, the maximum SINR beamformer will converge to the maximum SNR beamformer, because the term $\sum_{k=1}^{N} a_k a_k^*$ will approach the identity matrix. For five antenna elements, with 100 continuously transmitting users, off-diagonal terms of $\sum_{k=1}^{N} a_k a_k^*$ are still 20% of the values of diagonal terms. Therefore, in order for maximum SINR beamforming to approach maximum SNR beamforming, the number of users in cell needs to be very large.

The superiority of the maximum SINR method for the case of fewer than five users in Figure 4.5 and Figure 4.6 may be due to the fact that maximum SINR methods create nulls in certain directions when the number of interferers is small. This can cause a system realization where the SINR can be very high. As the number of users increases, this nulling effect disappears resulting in a performance as shown in Figures 4.5 and 4.6.

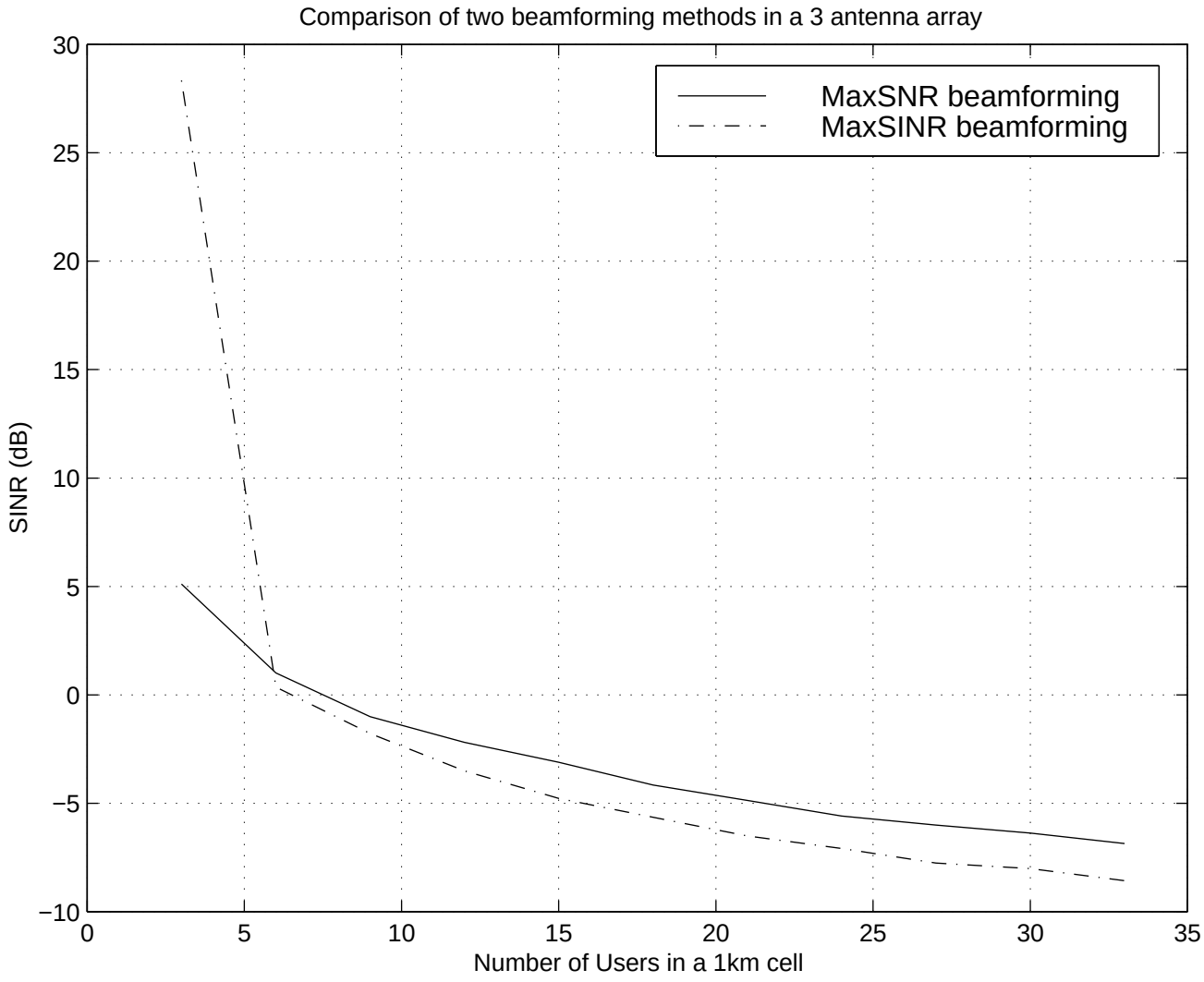

Figure 4.5: Performance comparison between maximum SNR and maximum SINR beamforming in the case of three antennas for three antennas. In maximum SINR beamforming, only the user locations within a cell are used in determining the weights.

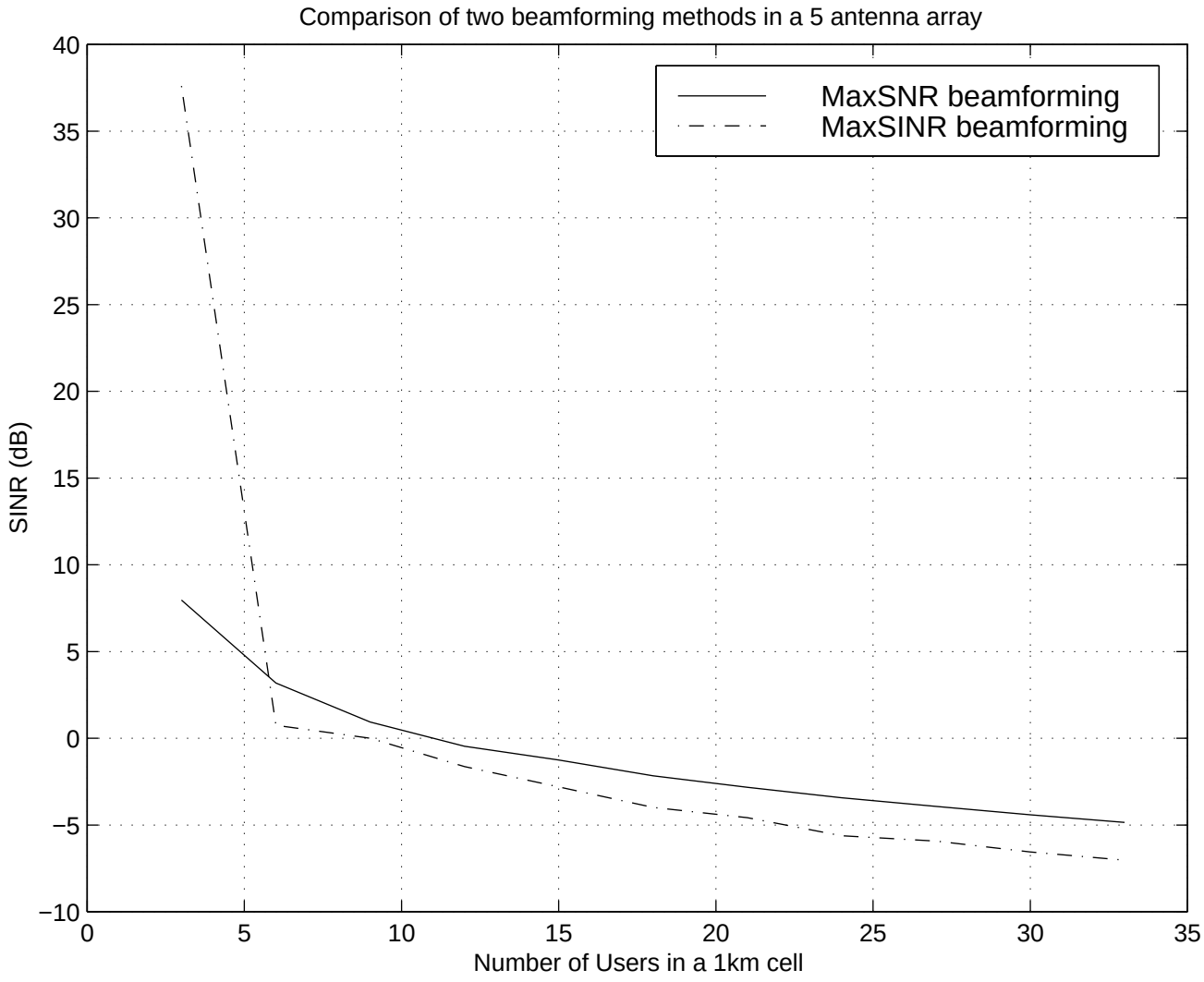

Figure 4.6: Performance comparison between maximum SNR and maximum SINR beamforming in the case of three antennas for five antennas. In maximum SINR beamforming, only the user locations within a cell are used in determining the weights.

4.6 Effect of Coverage on SINR performance

Mobile service providers need to provide the best possible service with the least cost. It is often useful to examine the trade off between increased base station density and performance. Higher base station density increases the service quality, but costs service providers more due to the cost of having more base stations. To study the effect of changing the cell radius, we fix the total power transmitted. Therefore, we assume that the total power transmitted per unit area is fixed.

Uncoded SINR performance is evaluated as a function of cell radius and base-station density. The results are plotted in Figures 4.7 to 4.10 for two scenarios, one with a 3 element circular array, one with a 5 element circular array. From Figures 4.7 and 4.8, as the base density increases, the SINR performance also improves.

Another way to characterize the area coverage is in terms of cell radius. Figures 4.9 and 4.10 show corresponding results to Figures 4.7 and 4.8 in terms of cell radius rather than base station density.

The figures also show that by using antenna arrays, we can increase the cell radius (i.e. reduced base-station density), and still achieve the same SINR performance, as in the case of a single antenna with a smaller cell radius.

For example, from Figure 4.7 to achieve -5dB of pre-despreading SINR, a base station density of $1.7/1\text{km}^2$ for one antenna element, $0.7/1\text{km}^2$ for three elements, and 0.4 base stations per 1km^2 for five elements is required. Similarly, from Figure 4.9, to achieve a -5dB SINR, the cell sizes are, 800m for one antenna, 1200m for three

antennas and 1500m for five antennas.

4.7 Summary

In this chapter, performance results of the channel estimator are presented, and the effects of steady state MMSE on system performance were studied. Using the CRV-based power control algorithm presented in Chapter 3, we studied the SINR performance as a function of the number of users, the beamforming method, the cell density and the cell radius. The results show that by using the proposed CRV-based power control algorithm for downlink power control and beamforming, we can increase the capacity and coverage, and decrease base station density. The results also show that having multiple cellular service levels available does not decrease the overall weighted SINR of the cell.

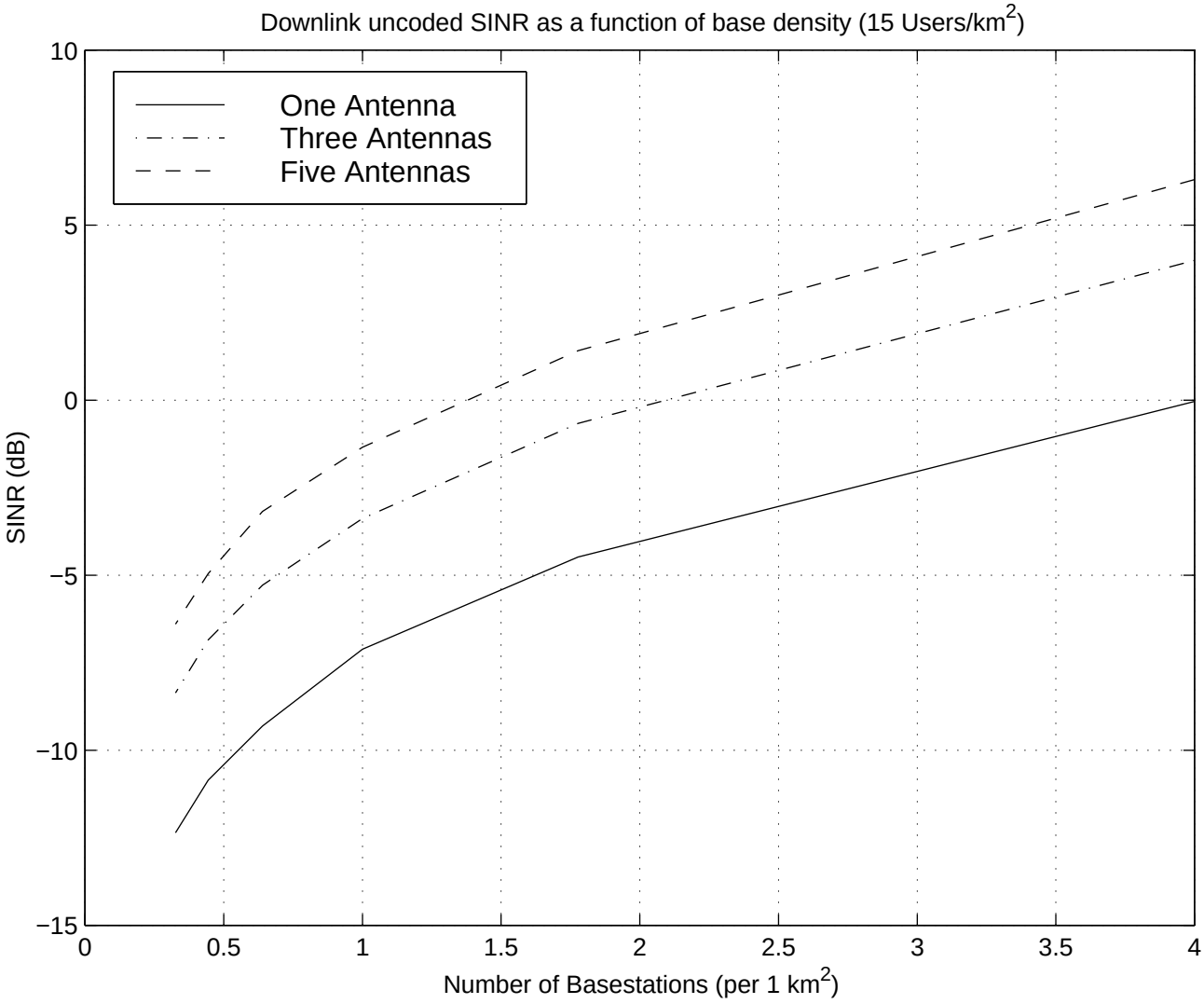

Figure 4.7: SINR as a function of base density with a mobile user density of 15 users/1km radius.

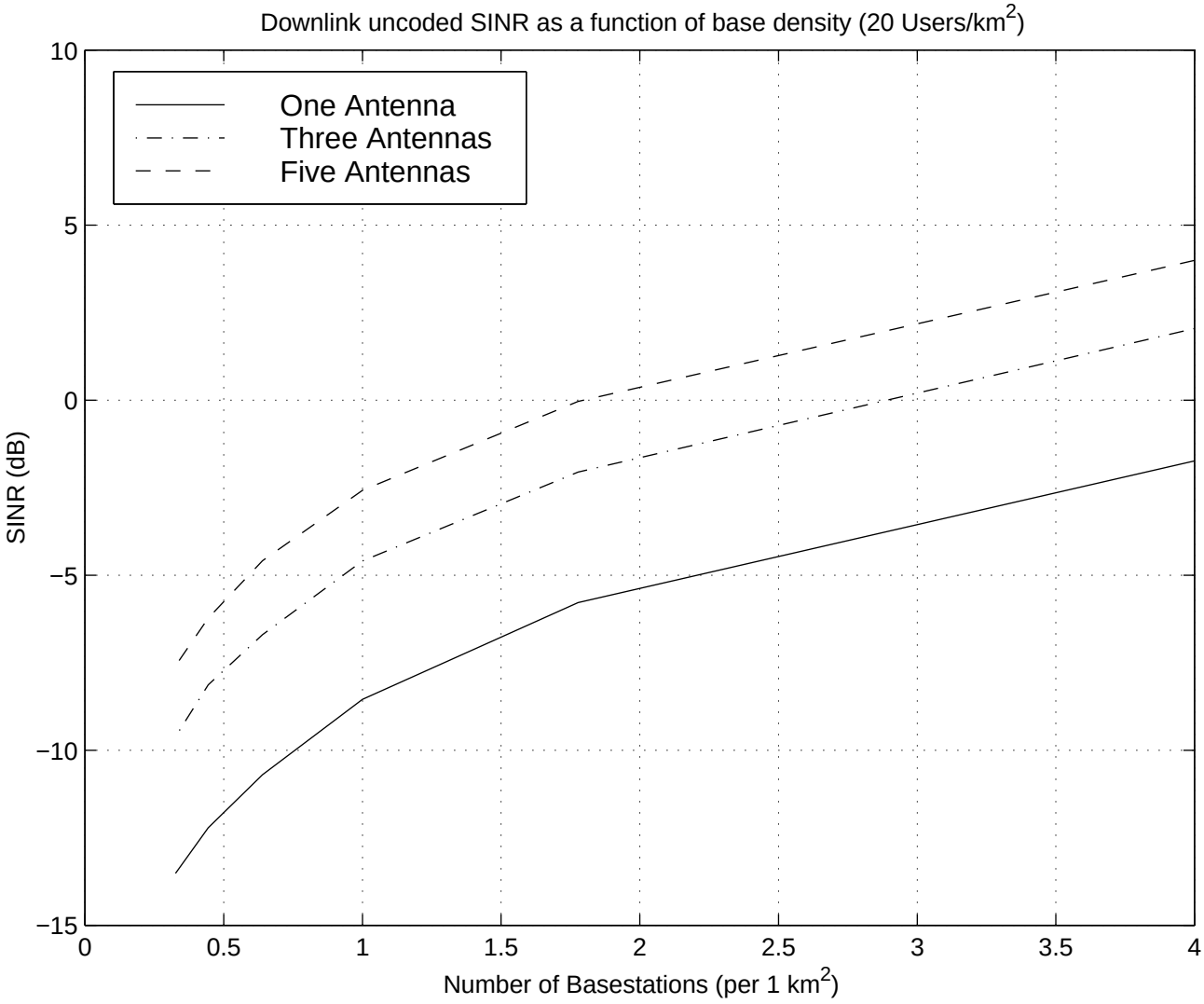

Figure 4.8: SINR as a function of base density with a mobile user density of 20 users/1km radius.

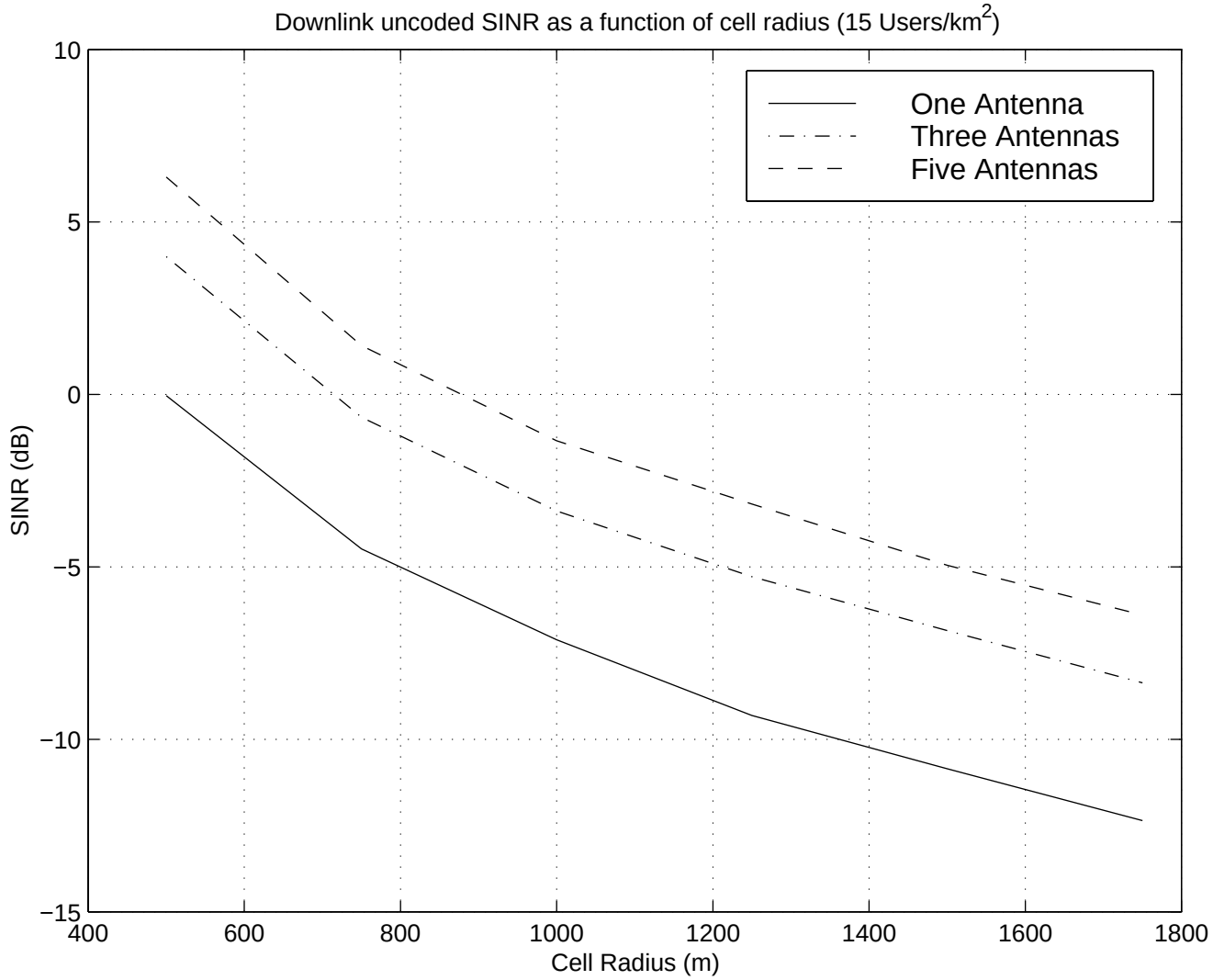

Figure 4.9: SINR as a function of cell radius with a mobile user density of 15 users/1km radius.

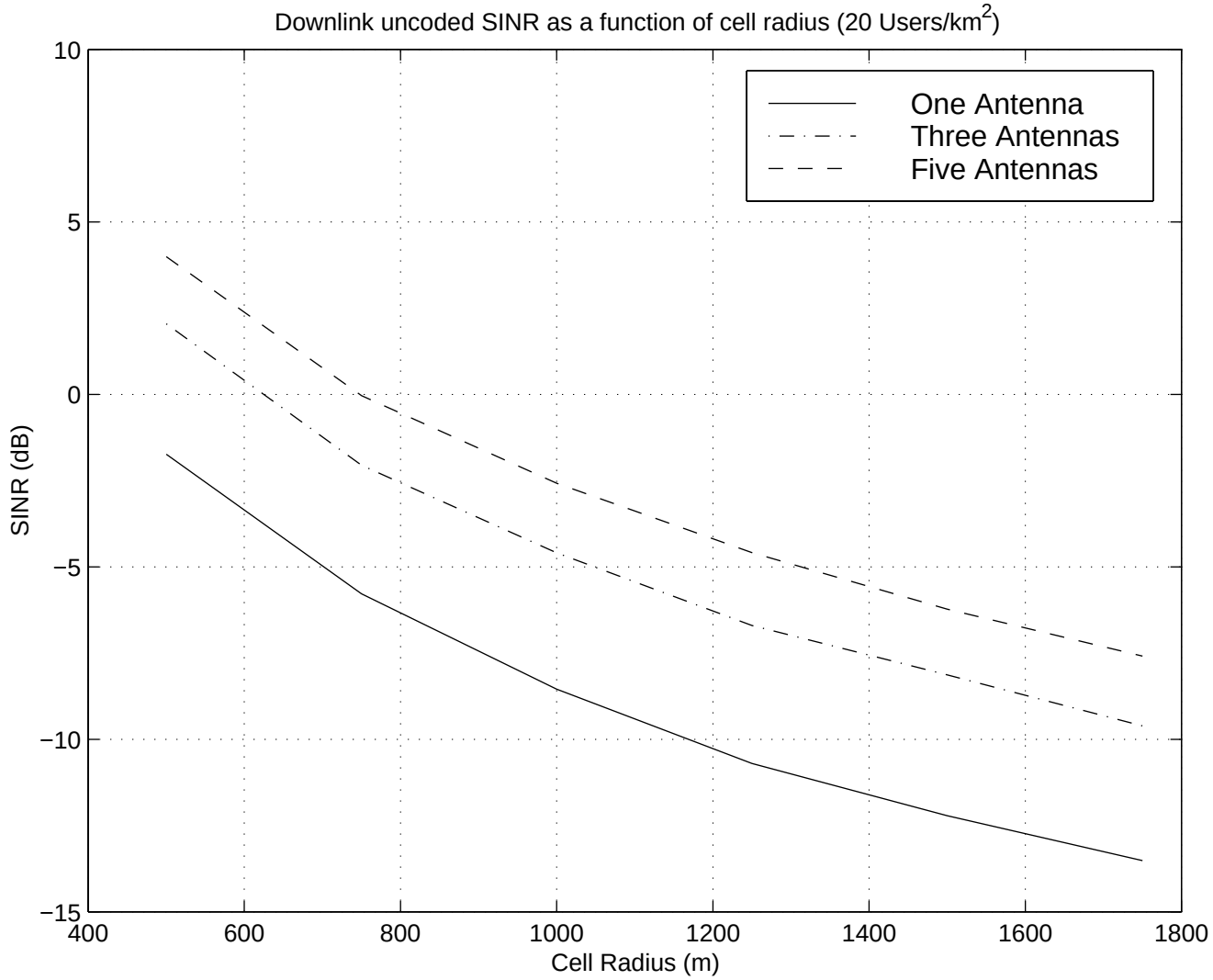

Figure 4.10: SINR as a function of cell radius with a mobile user density of 20 users/1km radius.

Chapter 5

Sequential Detection of Uplink Signals in Wideband CDMA Multipath Environment

5.1 Introduction

The use of wideband CDMA has been proposed for applications such as multimedia that require high bandwidth. To achieve these higher data rates, wideband CDMA uses higher chip rates. An increased chip rate means a reduced chip period. Therefore, many multipath components would be separated by more than one chip period, meaning that more resolvable paths are available for the receiver [50].

In CDMA environments where multipath propagation exists, RAKE receivers are often used to combat multipath interference [1] [33]. RAKE receivers increase the SNR by combining multipath components.

In wideband CDMA, a multipath component that travels an extra 100 meters will result in a delay of 333 ns, translating to a delay of 0.373 chips for the IS-95 chip rate, 1.67 chips for 5 Mcps chip rate and 5 chips for a 15 Mcps chip rate. Therefore, in wideband CDMA, the multipath delays are spread out over a larger number of chip periods than in IS-95 systems. Increasing the chip rate reduces the chip period, so small variations in the relative delays of multipaths could change the multipath delay parameters by several chips. As a result of the larger delay spread, the received signal must be correlated with many possible shifts in PN sequence with a resolution of a chip period or less over a large interval [49]. If the search space is significantly larger than the number of strong multipaths, the majority of the path delays will not yield significant energy. Therefore, if we can reduce the amount of computation used for obtaining multipath parameters which do not contain any signal, a faster receiver implementation may be realized.

Due to the spatial separation of users, coherent antenna array signal processing at the base station can be used to reduce multiple access interference and increase performance and capacity. Two-dimensional (spatial-temporal) RAKE receivers have been proposed to allow beamforming and combining of multipath components from different angles and delays [23]. With a mechanism to estimate a set of weights that differentiates signals based on channel response vectors (CRVs), a 2-D RAKE receiver can be implemented using a two-dimensional search through time and space. We refer this as a full-search 2-D RAKE receiver.

In the following sections, we propose an alternative receiver structure that forms

hypotheses that multipath components exist for each possible delay and CRV. A sequential hypothesis testing algorithm is used to reject delay/CRV parameter pairs that have a low probability of containing a signal. By rejecting parameters that have a low probability of containing a signal at an early stage, we can decrease the total number of calculations to be performed.

In traditional RAKE implementations, the number of RAKE fingers is fixed. For the proposed implementation, the total number of RAKE fingers varies depending on the time-varying propagation characteristics of the channel. The objective is to include all parameters that have a high probability of containing a signal in the RAKE combiner.

5.2 Background

In CDMA systems, multipath components have the property that the delayed versions of a signal are mutually uncorrelated as long as the relative delay is greater than one chip period. This is due to the statistical properties of PN sequences that modulate the transmitted signal. Therefore, if an antenna array is employed, we can process each delayed signal separately if we know the correct delay, amplitude and CRV [29].

5.2.1 Multipath Parameter Estimation for DS-CDMA Signals

One method to determine the delay, amplitude, and CRV is to enumerate the set of all possible parameters, and search the parameter space for space-time parameters

that minimize the distance between an ideal reference signal and the received signal. *A priori* information on the number of multipaths is often assumed known. The search can be done in both the frequency and time domains [48] [36]. Methods using frequency domain analysis require high SNR. When there are multiple users, the interference power will be high, reducing the performance of frequency-domain based least-squares estimates. If the signal is despread to increase the SNR, multipath signal components will be lost. Frequency domain algorithms usually require a set of weights to be pre-calculated for creating spatial nonoverlapping sectors via beamforming [48].

In general, since the number of simultaneous users present in a CDMA system is greater than one, frequency-domain processing without eliminating interfering users will yield poor performance. Time-domain search generally involves decorrelating the received signal with all possible shifted versions of the PN sequence, and estimating the delays based on the result [49]. The despreading or decorrelation process is computationally expensive when the number of possible paths and the number of users are large.

An alternative method is to treat the problem of estimating the multipath parameters as a hypothesis testing problem. Assuming that we have an accurate estimate of the number of users in the cell as well as their spreading sequences, we can generate hypotheses for all possible shifts of the PN sequence over a given time interval. The received signal is then used to test these hypotheses. Naguib proposed in his 2-D RAKE the use of a threshold detector after initial beamforming to determine whether a multipath signal exists [23] over each delay period. This is effectively a hypothesis

testing solution. However, we will show that the testing of all possible shifts of PN sequences can be achieved efficiently through the use of a sequential detection scheme to reduce the computational complexity.

5.2.2 Optimum Combining of Multipath Signals

To optimally combine the received multipath signals, a maximum ratio combiner (MRC) would maximize the output SNR [5]. In MRC, the receiver knows the correct delay and signal strength of each multipath. The output of the chip-matched filter corresponding to a particular delay will be weighted according to its complex signal strength and all multipath components are summed to generate the decision statistic.

An alternative to MRC is the RAKE structure [33]. We can model the effects of a multipath channel as a tapped delay line with statistically independent time varying tap weights [33]. The RAKE structure first performs chip-matched filtering for each tap delay and then weights the output of each chip-matched filter with the signal strength for that tap. If the channel tap weights are estimated perfectly, then the output decision statistic of a RAKE combiner is equivalent to the MRC [33]. Therefore, the optimum performing of a RAKE receiver will have the same output SNR as a MRC.

In the RAKE structure, the receiver attempts to collect energy from multipath components that fall within the time interval T_c (See Figure 5.1. It is assumed that each delay tap will contain some signal energy. Tap correlators containing only noise

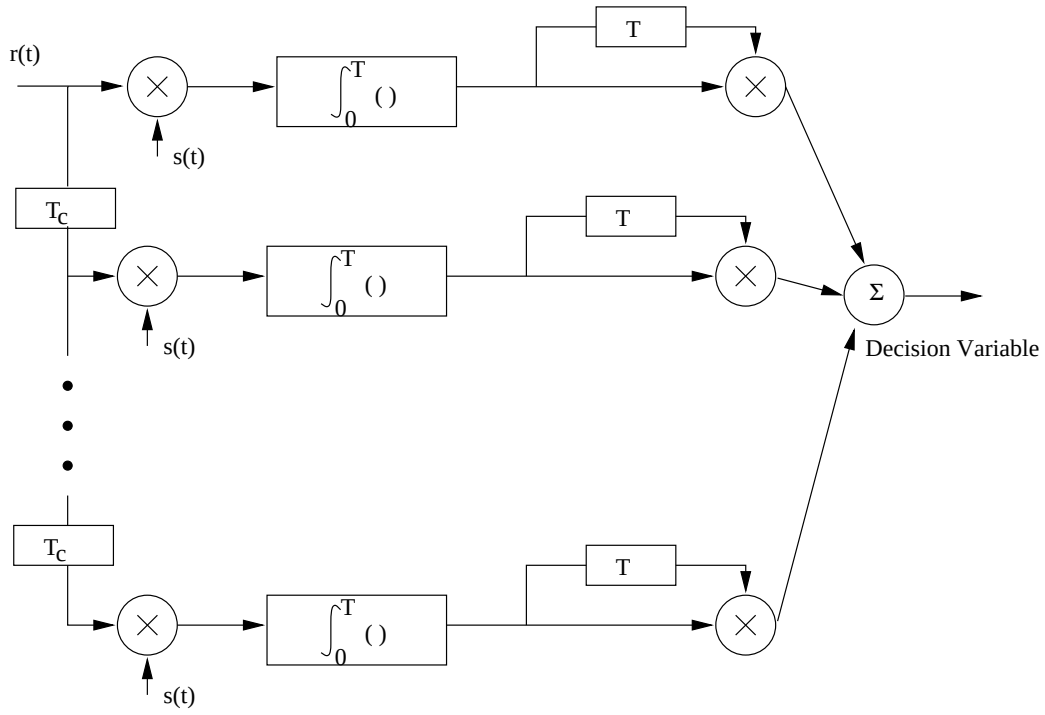

Figure 5.1: RAKE demodulator for DPSK signals.

should not be included in RAKE combining [33]. Each of these taps is often referred to as a *finger* of the RAKE receiver. Like MRC, the RAKE structure uses the complex amplitude to weight each finger.

The system block diagram of a realization of the RAKE receiver is shown in Figure 5.1.

5.3 Uplink Channel Model

In this section, we consider the multipath uplink channel, including fading and shadowing effects. It is also assumed that perfect power control is used for the generic

CDMA environment, such that the average power for the dominant path is constant. For the base station, an antenna array is used to allow spatial processing, and for simplicity, BPSK modulation is assumed. The number of elements in the antenna array is M.

First, consider the signal component from one mobile. The digital baseband transmitted signal for i^{th} mobile using PN sequence $\tilde{c}_i(n)$ can be expressed as:

$$x_i(n) = WC(d_i(n))\tilde{c}_i(n), \quad i = 1, 2, \cdots, N \tag{5.1}$$

where $d_i(n)$ is the bit transmitted by the mobile and is constant over one symbol period, $WC(d_i(n))$ is the walsh code corresponding to the data bit $d_i(n)$, n is the discrete time index and N is the number of users in the cell. By combining walsh code and the PN sequence into one sequence, we can be write (5.1) as,

$$x_i(n) = c_i(n), \quad i = 1, 2, \cdots, N \tag{5.2}$$

Assume that the channel memory caused by the effects of multipath propagation can be modeled as an FIR system [22] with a maximum delay spread of T_d chips. We can write the channel for the i^{th} user as:

$$h_i(n) = \sum_{j=1}^{L} a_{ij}\delta(n - \tau_{ij}) \tag{5.3}$$

where the index j represents one of L multipaths experienced by the i^{th} user and τ_{ij} is the integer chip time delay for the multipath. It is assumed that L is not known.

The received digital signal at the base station with N users, $\mathbf{r}(n)$, is:

$$\mathbf{r}(n) = \sum_{i=1}^{N}\sum_{l=1}^{L} \mathbf{a}(\theta_{il})x_i(n - \tau_{il}) + \upsilon(n) \tag{5.4}$$

where $\mathbf{a}(\theta_{il})$ is the CRV of the l^{th} multipath of the i^{th} mobile. The quantity $v(n)$ represents additive white Gaussian noise.

5.4 Time Domain Detection of Multipath Signals

To find the multipath delay and path attenuation parameters, most algorithms solve an optimization problem. For time-domain-only RAKE receivers, Liu and Zoltowski in [22] proposed a method to estimate the optimum weights for a RAKE receiver at a one chip resolution by solving a linear system of NT_d equations. When the number of users, N, and largest possible delay, T_d, are large, the process is very computationally intensive. In the following approach, we implement the spatial-temporal RAKE where beamforming is performed using a pre-generated set of weights.

First we describe the detection of multipath signals without beamforming. The received signal after correlation with the PN sequence of the i^{th} mobile with integer delay τ_{ij} of the j^{th} path, is denoted by $Z_{i,j}$,

$$\begin{aligned} Z_{i,j} &= \sum_{n=1}^{G} r(n)c_i(n-\tau_{ij}) && (5.5)\\ &= a_{ij}d_iG + \sum_{n=1}^{G}\sum_{k=1}^{N}\sum_{\substack{l=1\\k,l\neq i,j}}^{L}\left(a_{kl}d_kc_k(n-\tau_{kl})+v(n)\right)c_i(n-\tau_{ij}) && (5.6)\\ &= a_{ij}d_iG + IN_{ij} && (5.7)\end{aligned}$$

where (5.4) is used and where,

$$IN_{ij} = \sum_{n=1}^{G}\sum_{k=1}^{N}\sum_{\substack{l=1\\k,l\neq i,j}}^{L}\left(a_{kl}d_kc_k(n-\tau_{kl})+v(n)\right)c_i(n-\tau_{ij}) \qquad (5.8)$$

The signal from the i^{th} mobile with shift τ_j will have a processing gain of G chips per bit, and interference from other users can be modeled as additive white Gaussian interference [33]. The correlation statistic $Z_{i,j}$ can be used to test for the presence of the signal delayed by jT_c seconds from the i^{th} mobile. Define H_{ij} as the hypothesis that there exists a strong path at the j^{th} delay for the i^{th} mobile. Modeling the effects from interfering users using a Gaussian approximation [35], we can use the following decision rule:

$$Z_{i,j} \begin{cases} < a_G & \text{no signal present} \\ \\ \geq a_G & \text{signal present} \end{cases} \tag{5.9}$$

where the threshold a_G will depend on the design criterion and the probability distribution of the interference and noise.

If the hypothesis H_{ij} is true, then the correlation statistic $Z_{i,j}$ is directly related to the signal strength from the j^{th} path of the i^{th} mobile. Otherwise, we assume that there is zero signal strength arriving from the j^{th} multipath. In effect, a cut-off is chosen such that only a multipath component with the correlation statistic above threshold a_G is to be included in the RAKE receiver. A RAKE receiver using a threshold detector is shown in Fig. 5.2.

The test statistic $Z_{i,j}$ can belong to one of two mutually exclusive subsets, Γ_0 and Γ_1 of the observation space. Let

$$Z_{i,j} \in \Gamma_0 \qquad \text{if no signal present} \tag{5.10}$$

$$Z_{i,j} \in \Gamma_1 \qquad \text{if signal present} \tag{5.11}$$

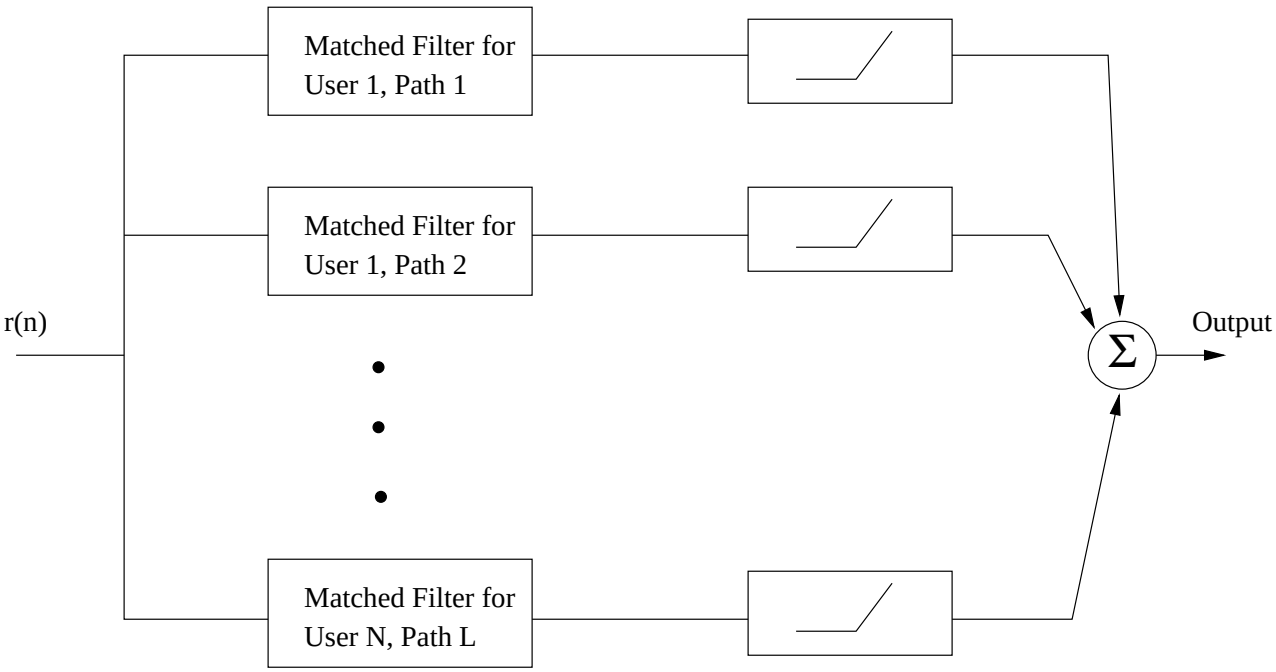

Figure 5.2: RAKE receiver with threshold detector.

5.4.1 Truncated Sequential Detection of Multipath Signals

A search for a large number of hypotheses where the vast majority contain no signal consumes significant resources if a full search were to be used. The problem of PN acquisition for narrowband CDMA has been studied by Tantaratana [41], who proposed the use of sequential detection for the case of a single antenna. In [41], a design algorithm for a sequential detector based on Wald's approximation [45] is presented. In [15], a sequential acquisition scheme is shown have a shorter acquisition time than a non-sequential acquisition scheme. Both designs utilize Wald's approximation [45]. Wald's approximation uses the union bound to design sequential test thresholds that guarantee a specified probability of false alarm and probability missed detection. In this section we will apply sequential detection using additive noise to model multiuser

interference.

Instead of deciding after G samples whether $Z_{i,j}$ contains a signal or not, a sequential test with a maximum number of stages, G, can be used. Define the individual multiplicative term in the correlation metric at stage k of the test for signal presence in $Z_{i,j}$ as $\chi_{i,j}(k)$:

$$\chi_{i,j}(k) = r(k)c_i(k - \tau_{i,j}) \tag{5.12}$$

where $r(k)$ is the received signal and let

$$Z_{i,j} = \sum_{k=1}^{G} \chi_{i,j}(k) \tag{5.13}$$

If we assume that the interference from other mobiles and multipath interference can be modeled as Gaussian, then,

$$\chi_{i,j}(k) \sim \begin{cases} \mathcal{N}(0, \sigma_{i,j}^2) & \text{if a signal path does not exist} \\ \mathcal{N}(a_{ij}, \sigma_{i,j}^2) & \text{if a signal path exists} \end{cases} \tag{5.14}$$

where $\sigma_{i,j}^2$ contains both interference and additive thermal noise experienced by the j^{th} path of the i^{th} user. Since the thermal noise and interference are uncorrelated, we have that

$$\sigma_{i,j}^2 = Var\{IN_{i,j}\} + \sigma_t^2 \tag{5.15}$$

where σ_t^2 is the additive thermal noise variance.

The decision at stage K $(1 \leq K < G)$ of the test can be written as:

$$\sum_{k=1}^{K} \chi_{i,j}(k) \begin{cases} < b_K & \Rightarrow \text{choose } H_0 \text{ and terminate test} \\ \text{otherwise} & \Rightarrow \text{continue to stage K+1} \end{cases} \tag{5.16}$$

At the G^{th} stage, the test is terminated, i.e. a final decision is reached,

$$Z_{i,j} = \sum_{k=1}^{G} \chi_{i,j}(k) \begin{cases} < b_G & \Rightarrow \text{choose } H_0 \text{ and terminate test} \\ \text{otherwise} & \Rightarrow \text{choose } H_1 \text{ and terminate test} \end{cases} \tag{5.17}$$

The thresholds b_K, $1 \leq K \leq G$ in (5.16) and (5.17) can be determined via the method in [32]. The design in [32] guarantees that for independent and identically distributed samples, as is the case in this problem, a probability of false alarm less of than α, and a probability of missed detection of less than β for $1 \leq K < G$. From [32],

$$b_K = \frac{\beta}{1-\alpha}\sigma^2 + K\frac{E\{a_{ij}\}}{2} \tag{5.18}$$

In (5.18), α and β are the probability of false alarm and the probability of missed detection, respectively. The quantity, $E\{a_{ij}\}$ is the mean signal strength for a multipath component.

The sequential test will reject a particular hypothesis if the statistic at stage K falls below the threshold b_K, thereby reducing the number of calculations necessary when the null hypothesis, H_0, is true. The hypothesis that survives to the G^{th} stage will be treated as a resolvable path, and the final test statistic, $Z_{i,j}$, will be treated as the correlation statistic for that multipath, which can be used later for maximal ratio combining [5] in the RAKE receiver.

5.4.2 Mean Test Length for a Sequential Hypothesis Test

The mean test length for a sequential hypothesis test in an additive Gaussian environment was calculated by Blostein and Huang in [4]. A summary is provided below.

Let the single-variable Gaussian probability distribution function be defined as $f(x)$,

$$f(x) = \frac{1}{\sqrt{2\pi\nu}} \exp\left[-\frac{1}{2}\left(\frac{x-\lambda}{\nu}\right)^2\right] \tag{5.19}$$

Define

$$r_i \equiv \Pr(\text{Sequential Test Reaching } i^{th} \text{ stage}) \tag{5.20}$$

Initially, the distribution of the test statistic is Gaussian. For a one-sided sequential probability ratio test (SPRT), the upper threshold is infinite [41], and the lower threshold is b_i for stage i. After each stage, the test may be terminated if the statistic falls below the threshold b_i, $1 \leq i \leq G$. Therefore the distribution of the test statistic at stage i, $f_i(x)$, is

$$f_i(w) = \int_{b_{i-1}}^{\infty} f(w-x) f_{i-1}(x) dx \tag{5.21}$$

The probability of reaching the i^{th} stage involves integrating the distribution, $f_{i-1}(x)$ from the lower threshold to the upper threshold, which in this application is infinity.

The mean test length can be found as,

$$E\{Test\ Length\} = \sum_{i=1}^{K} r_i \tag{5.22}$$

$$= \sum_{i=1}^{K} \int_{b_{i-1}}^{\infty} f_{i-1}(x) dx \tag{5.23}$$

Equation (5.23) cannot be evaluated in closed-form. Instead, numerical integration methods such as Simpson's rule can be used to approximate the integral.

5.5 Spatial Domain Detection of Multipath Signals

When there are multiple antenna elements at the base station, the received signal is formed by spatial beamforming at each time delay prior to diversity combining. If we have a pre-selected set of weights, one for each sector in the cell, we can form a signal-present hypothesis for each possible delay in each sector.

Generalizing the results from the previous section, the test statistic of the j^{th} path of the i^{th} user using the k^{th} set of spatial beam weights can be expressed as,

$$Z_{ijk} = \mathbf{w}_k^* \mathbf{a}_{ij} G + IN_{ijk} \tag{5.24}$$

$$IN_{ijk} = \sum_{n=1}^{G} \sum_{\substack{m=1 \\ m,l \neq i,j}}^{N} \sum_{l=1}^{L} \mathbf{w}_k^* \mathbf{a}_{kl} d_k c_m(n - \tau_{ml}) c_i(n - \tau_{ij}) + v(n) \tag{5.25}$$

where $v(n)$ is the additive thermal noise, $\mathbf{w}_k$ is the beamforming weight vector for the k^{th} sector, c_i is the chip for the i^{th} user, i and τ_{kl} is the delay for the l^{th} path in sector k.

Hypothesis testing can be performed on Z_{ijk} as in the previous section. However, the computational efficiency can be further improved by performing the testing in two stages, the first in the time domain, and the second in the spatial domain.

5.5.1 Tree Structured Spatial Search of Multipath Signals

If a particular time delay contains a signal, we would like to decide on the spatial sector(s) where the signal resides. To locate the spatial sector where the signal resides, we can use a binary tree structured search. First, we determine whether if the signal is coming from half of the sectors in the set. If the decision statistic is great than the threshold κ_1, we reject the hypothesis the signal is coming from those sectors. Alternatively, if the decision statistic is above the threshold, we can further subdivide the set of sectors to one quarter the size of the original set. We may repeat this process recursively until individual sectors are being tested. By rejecting a particular set of sectors as containing signal in an early depth level, we can reduce the total amount of computations performed.

To identify each node at a particular depth level of the tree search, we define the following rule:

> Labeling Rule
> To subdivide the set of sectors in node q at depth level p, label the resulting two subsets at depth level $p+1$ as nodes $2q-1$, $2q$, respectively.

As an example of the labeling rule, we assign the node number and tree depth for a 4-sector search in Figure 5.3.

Define the set of sectors included at the q^{th} node of the p^{th} depth level as $\Theta_{p,q}$. Also, define the probability of accepting a hypothesis at stage p for the q^{th} node as

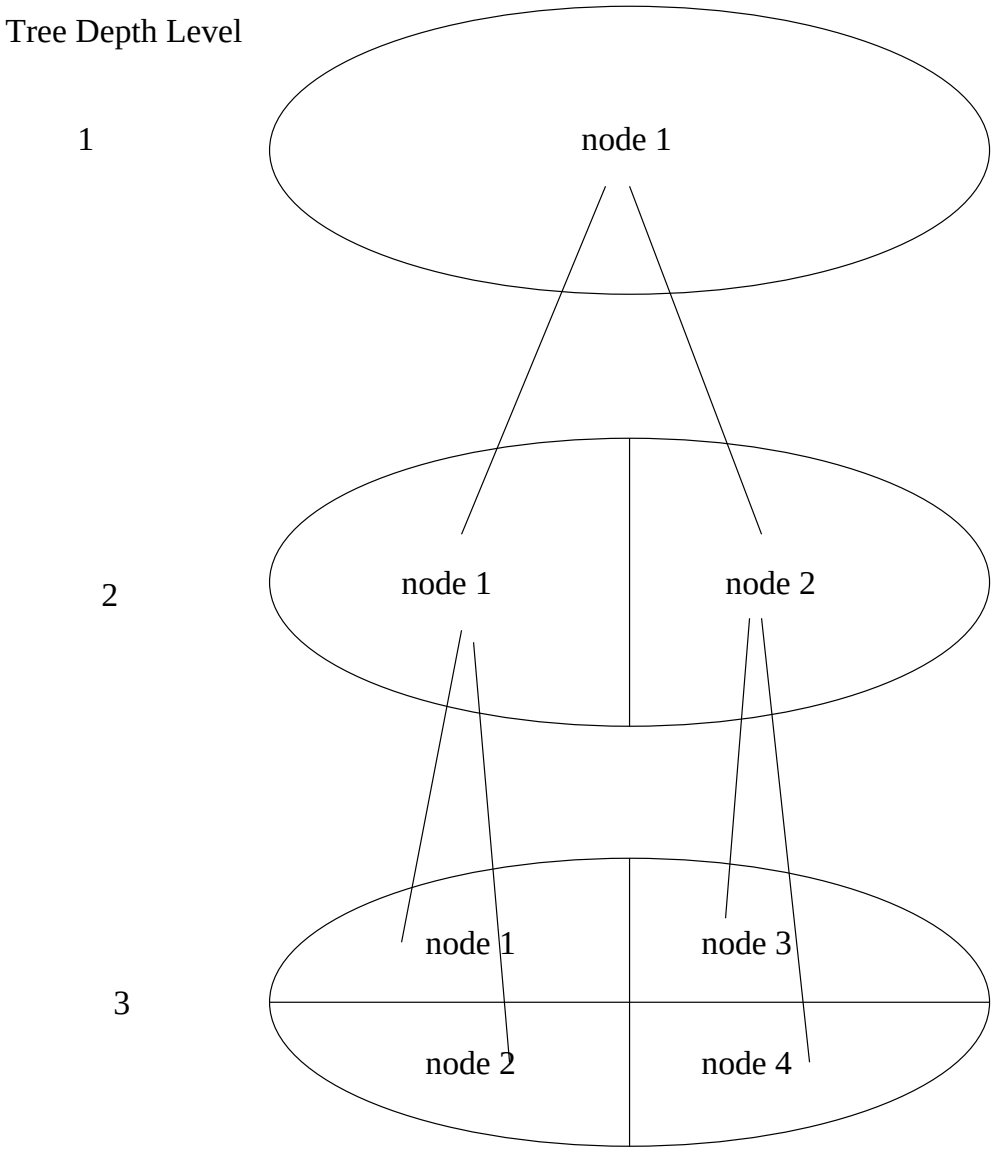

Figure 5.3: Example of assigning node numbers and tree depths in a 4-sector search.

δ_p^q. Therefore,

$$\delta_p^q = \Pr\{\text{accept that a signal is present in } \Theta_{p,q} \text{ at depth level p }\} \quad (5.26)$$

$$1-\delta_p^q = \Pr\{\text{reject that a signal is present in } \Theta_{p,q} \text{ at depth level p}\} \quad (5.27)$$

The test statistic for each depth level of the test consists of summing all the statistics Z_{ijk} for sectors in $\Theta_{p,q}$. The test statistic for the q^{th} node of the p^{th} depth level for the i^{th} user and j^{th} path can be expressed as:

$$Z_{i,j}^{p,q} = \sum_{k \in \Theta_{p,q}} Z_{ijk} \quad (5.28)$$

The decision for the q^{th} node of the depth level p is,

$$Z_{i,j}^{p,q} < \kappa_p \qquad \text{if there is no signal present} \quad (5.29)$$

$$Z_{i,j}^{p,q} \geq \kappa_p \qquad \text{if a signal is present} \quad (5.30)$$

where κ_p is the threshold for the depth level p in the spatial tree search. In the event that a signal is present, the test continues to the next depth level. Define the indicator function for the time-space correlation statistic at the q^{th} node of the p^{th} depth level as $I_{i,j}^{p,q}$,

$$I_{i,j}^{p,q} = \begin{cases} 0 & \text{if } Z_{i,j}^{pq} \text{ is decided to not contain a signal} \\ 1 & \text{if } Z_{i,j}^{pq} \text{ is decided to contain a signal} \end{cases} \quad (5.31)$$

Therefore, the indicator function will yield zero if the test is truncated at the node, and unity if it continues to the next depth level. At the final depth level of the test, the hypothesis is accepted or rejected.

The algorithm for the tree structured search is given in Figure 5.4.

```
/* The sectors that make up node q in the p^th depth level */
/* will containing multipath signals that have */
/* I_{i,j}^{p,q} = 1 and test statistic Z_{i,j}^{p,q} */

Initialize all I_{i,j}^{p,q} to 0

/*Initiate the tree structured spatial search for user i path j */
Test I_{i,j}^{1,1}


function Test I_{i,j}^{p,q}
/* returns the indicator function and the decision statistic */
   let Z_{i,j}^{p,q} = sum_{k in Theta_{p,q}} Z_{ijk}
   if Z_{i,j}^{p,q} > kappa_p
      if p < maximum depth level
         Test I_{i,j}^{p+1,2q-1}
         Test I_{i,j}^{p+1,2q}
      return 1
   else
      return 0
```

Figure 5.4: Algorithm for spatial tree search.

The test performed at each depth level of the spatial search is a fixed-length test. The tests are designed to yield a low probability of missed detection. As the spatial search narrows, fewer and fewer branches of the tree will survive.

5.5.2 Design of Thresholds for Spatial Tree

The test statistics for each depth level of the tree are not independent of the test statistics for the lower depth level. The test statistic at the q^{th} node of the p^{th} depth level, $Z_{i,j}^{p,q}$, contains the test statistic for the $(p+1)^{th}$ depth level such that,

$$Z_{i,j}^{p,q} = Z_{i,j}^{p+1,2q-1} + Z_{i,j}^{p+1,2q} \tag{5.32}$$

Since we have mutually dependent samples between different depth levels, the SPRT is not applicable [32]. However, since all possible partitions of sectors in node q at each depth level p are mutually exclusive, the test statistics, $Z_{i,j}^{p,q}$ (where $1 \leq q \leq 2^p$), are mutually independent. This property of the test statistic allows us to determine the probability of detection given a set of thresholds, κ_p, for each depth level.

If, for a tree-structured search with maximum depth level of Υ, we are given a set of thresholds κ_p, where $1 \leq p \leq \Upsilon$, we can find the probability of missed detection using these thresholds. To find the probability of missed detection using these thresholds, we integrate over the region of acceptance defined by these thresholds.

Using (5.32), we can express the probability of acceptance of sector 1 (or, by symmetry, of any other sector) at depth level Υ as,

$\Pr(H_1$ accepted at any node at the depth level Υ given signal strength $\lambda)$

$$= \Pr\left(\bigcap_{p=1}^{\Upsilon} Z_{i,j}^{p,1} > \kappa_p\right) \tag{5.33}$$

$$= \Pr\left(\begin{array}{l} Z_{i,j}^{\Upsilon,1} > \kappa_\Upsilon, Z_{i,j}^{\Upsilon-1,1} > \kappa_{\Upsilon-1}, \\ Z_{i,j}^{\Upsilon-2,1} > \kappa_{\Upsilon-2}, \cdots, Z_{i,j}^{1,1} < \kappa_1 \end{array}\right) \tag{5.34}$$

$$= \Pr\left(\begin{array}{l} Z_{i,j}^{\Upsilon,1} > \kappa_\Upsilon, \\ Z_{i,j}^{\Upsilon,2} > \kappa_{\Upsilon-1} - Z_{i,j}^{\Upsilon,1}, \\ Z_{i,j}^{\Upsilon-1,2} > \kappa_{\Upsilon-2} - Z_{i,j}^{\Upsilon-1,1}, \\ \cdots, \\ Z_{i,j}^{2,2} < \kappa_1 - Z_{i,j}^{2,1} \end{array}\right)$$

$$= \int \cdots \int_{\bigcap_{p=1}^{\Upsilon} Z_{i,j}^{p,1} > \kappa_p} f\left(Z_{i,j}^{\Upsilon,1}, Z_{i,j}^{\Upsilon,2}, Z_{i,j}^{\Upsilon-1,2}, \cdots, Z_{i,j}^{2,2}\right) dZ_{i,j}^{\Upsilon,1} dZ_{i,j}^{\Upsilon,2} dZ_{i,j}^{\Upsilon-1,2} \cdots dZ_{i,j}^{2,2} \tag{5.35}$$

$$= \int_{\kappa_\Upsilon}^{\infty} \int_{\kappa_{\Upsilon-1} - Z_{i,j}^{\Upsilon,2}}^{\infty} \cdots \int_{\kappa_{\Upsilon-2} - Z_{i,j}^{\Upsilon-1,2}}^{\infty} f(Z_{i,j}^{\Upsilon,1}) f(Z_{i,j}^{\Upsilon,2}) f(Z_{i,j}^{\Upsilon-1,2}) \cdots f(Z_{i,j}^{2,2}) dZ_{i,j}^{\Upsilon,1} dZ_{i,j}^{\Upsilon,2} dZ_{i,j}^{\Upsilon-1,2} \cdots dZ_{i,j}^{2,2} \tag{5.36}$$

$$= \int_{\kappa_\Upsilon}^{\infty} dZ_{i,j}^{\Upsilon,1} f(Z_{i,j}^{\Upsilon,1}) \int_{\kappa_{\Upsilon-1} - Z_{i,j}^{\Upsilon,2}}^{\infty} dZ_{i,j}^{\Upsilon,2} f(Z_{i,j}^{\Upsilon,2}) \int_{\kappa_{\Upsilon-2} - Z_{i,j}^{\Upsilon-1,2}}^{\infty} dZ_{i,j}^{\Upsilon-1,2} f(Z_{i,j}^{\Upsilon-1,2}) \cdots \int_{\kappa_1 - Z_{i,j}^{2,1}}^{\infty} dZ_{i,j}^{2,2} f(Z_{i,j}^{2,2}) \tag{5.37}$$

Using a Gaussian approximation, $f(Z_{ij}^{pq})$ is a Guassian density. with mean λ and variance equal to the variance of IN_{ij}. The signal strength λ would equal a_{ij} if a signal is present, and zero if a signal is not present.

Using numerical integration, we can determine the probabilities of detection for different design thresholds. The threshold also determines the probability of false alarm at each depth level of the test, affecting the number of computations performed

by the system. In designing the spatial search, it is desirable to include as many multipath signals as possible. Therefore, the thresholds should be designed to have a high probability of detection.

To design the test thresholds, we have to find a choose a set of thresholds that satisfy a certain probability of detection. We can start with an arbitrary set of thresholds and iteratively improve the thresholds to achieve a specific probability of detection by numerically integrating (5.37). To reduce the amount of iteration neccessary to achieve a satisfactory design, we can approximate (5.37) by adding extra mass to the integration as seen in (5.38). Since additional probability mass is added, the approximated probability value would always be lower than the actual value found using (5.37).

$$\begin{aligned} &\Pr(H_1 \text{ accepted at the depth level } \Upsilon \text{ for a given signal strength } \lambda \text{ }) \\ \approx\ & \int_{\kappa_\Upsilon}^{\infty} dZ_{i,j}^{\Upsilon,1} f(Z_{i,j}^{\Upsilon,1}) \int_{\kappa_{\Upsilon-1}}^{\infty} dZ_{i,j}^{\Upsilon,2} f(Z_{i,j}^{\Upsilon,2}) \int_{\kappa_{\Upsilon-2}}^{\infty} dZ_{i,j}^{\Upsilon-1,2} f(Z_{i,j}^{\Upsilon-1,2}) \\ & \cdots \int_{\kappa_1}^{\infty} dZ_{i,j}^{2,2} f(Z_{i,j}^{2,2}) \end{aligned} \tag{5.38}$$

Since the thresholds are no longer dependent on the previous integral, we can evaluate each integral separately in (5.38), thereby increasing the speed of iteration. We then modify the thresholds to achieve the same probability of detection using the exact expression in (5.37).

5.6 RAKE Receiver Performance

The SNR performance of the RAKE receiver will depend on how many signal components are detected. A path from the j^{th} delay and user i has SNR_{ij} given by,

$$SNR_{ij} = \frac{a_{ij}^2 G}{IN_{ij}\varphi_{array}} \tag{5.39}$$

where φ_{array} is the attenuation of the interference due to beamforming of the received signal. An analysis on the effects of beamforming on interference reduction can be found in [8].

The resulting ideal SNR for the i^{th} user that can be achieved with L multipath components,

$$SNR_i = \sum_{j=1}^{L} SNR_{ij} I_{ij}^{pq} \tag{5.40}$$

Note that the indicator function is used to include the SNR from components not rejected during our hypothesis testing algorithm.

The algorithm performs suboptimally as compared to the ideal combiner if signal components are rejected during hypothesis testing. Optimum performance is achieved through higher computational costs, since no delay-sector hypothesis pairs can be rejected. By using a RAKE structure, we can achieve the same output SNR as an MRC [33]. In the RAKE structure, multipath weights are determined by their signal strength and phase, often by long term averaging [27] [33]. In results presented in this chapter, we assume that signal strength and phase are known perfectly to calculate the output SNR. The output SNR of a RAKE receiver is the sum of the SNRs of

each individual tap. If the signal strength is modeled as a random variable, rejection of weak signal paths does not significantly affect the overall SNR.

5.7 Computational Complexity of the Proposed RAKE Receiver

The goal of using a sequential detector is to dismiss the noise-only hypothesis quickly [39]. We now show that we can reduce the amount of computation required to process hypotheses in which no signal is present without significantly reducing the performance benefits of a RAKE structure.

The computational complexity can be measured by the number of multiplications and summations that are performed by the algorithm compared to that of a full chip-matched filter. We will compare the mean test length of the sequential detector as well as the number of operations required for tree search for a given set of design parameters to a "brute-force" full chip-matched-filter implementation.

5.8 Numerical Results and Simulations

To test the performance of a 2-D RAKE receiver utilizing sequential detection, we use both numerical calculations and Monte Carlo simulation. For Monte Carlo simulation, random data bits are spread by a 256-bit PN sequence using the IS-95 short code to

modulate random data from each user. The received signal is the sum of all the user's multipath components. The multipath components are generated with random path attenuation and delay. The path attenuation a_{ij} for each multipath component comprises the overall effects of fading and shadowing. It is assumed power control is used to offset the near-far effect, and ensure that the dominant path have constant average power. We can normalize the desired average power to be one, therefore the expected value of a_{ij} is one. To simulate the effects of an antenna array, each path will be assigned a CRV based on the array response of an ideal circular array for a randomly generated angle. The arrival angle is assumed to be uniformly distributed. In this section, we study a cellular environment with 10 continuously transmitting users, each transmitting four independent multipaths.

The signal strength from each component will be a random variable that is Rayleigh distributed. The path delay is uniformly distributed. The signal waveform is assumed to have square pulses. It is assumed in our performance analysis that four paths exist over 10μs.

In this section, we first present numerical results using Monte Carlo simulation. Then the results for test length and SINR performance are verified using theoretical calculations.

5.8.1 Various Receiver Designs

In this subsection, we will present several different designs, including a conservative design which performs as well as the full search RAKE receiver at a high computational cost, a more practical design with a slight trade-off in performance for a high reduction in complexity, and a third design that sacrifices more SNR performance for an even larger reduction in complexity. The important design parameter for the sequential probability ratio test (SPRT) is given by,

$$b = \frac{\beta}{1-\alpha} \tag{5.41}$$

where α, β are the probabilities of false alarm and missed detection, respectively. A lower value of b yields a more conservative design, corresponding to smaller values of α and β.

From (5.18) and (5.41), the thresholds for stage, K, of the SPRT are given by,

$$b_K = bVar\{IN_{ij}\} + K\frac{E\{a_{ij}\}}{2} \tag{5.42}$$

where IN_{ij} is the interference plus noise given by (5.8) and a_{ij} is the signal strength for each multipath. The maximum number of stages is assumed to be 256 which corresponds to the number of chips per symbol.

We assume that a slow power control algorithm would have the effect of offseting the near-far effect for each user. For each user, the multipath attenuation a_{ij} is an independent random variable that is Rayleigh distributed with mean one and variance one. The variance of the interference and noise is dependent on the number

of users. We assume the interference from each user and their multipaths are mutually independent. For N users with L multipaths,

$$Var\{IN_{ij}\} = NLE\{a_{ij}^2\} + \sigma_t^2 \tag{5.43}$$

where σ_t^2 is the uncorrelated thermal noise term.

In the spatial search stages corresponding to sector tree depth levels, the individual thresholds for each depth level p, κ_p, need to be determined. It is assumed that a set of 32 weight vectors are available for beamforming using 32 (2^5) sectors. A binary tree with 5 depth levels is therefore used for the search.

To initialize the iterative threshold search procedure, we use (5.38) to find approximate values of κ_p that would satisfy a particular probability of detection. Then by adjusting the approximate thresholds, we use (5.37) to ensure that the final thresholds chosen would satisfy a particular probability of detection.

Using the above method, we have designed the following tests:

A conservative design (design #1) essentially performs an exhaustive search. For the temporal search stage, the SPRT design parameter b has a value of 0.1, corresponding to a probability of detection of 0.99 and rejecting a noise-only component of 0.1 (probability of false alarm equal to 0.9). For the spatial search, the thresholds are iteratively designed to give a probability of detection to within 0.005 of of 0.99. The designed thresholds are shown in Table 5.1.

A lower complexity receiver design (design #2) shown in Table 5.2. A temporal SPRT design parameter b of 0.4 was chosen. This choice of b would result in a false

alarm probability of 0.75 and a probability of detection of 0.9 in the temporal search. The spatial search thresholds are designed for a probability of detection of 0.90.

An alternate test design (design #3) that achieves higher computational reduction is shown in Table 5.3. The SPRT design parameter b used was 0.7, corresponding, for example to a temporal false alarm probability is 0.35 and a probability of detection of 0.75. The spatial search was designed for a probability of detection of 0.75.

Since the spatial search has 5 depth levels, the set of thresholds designed for each probability of detection is not unique. For example, if we change the threshold κ_1, we can adjust the threshold κ_2 such that the resulting probability of detection remains the same.

5.8.2 Monte Carlo Results

For the full-search RAKE receiver, assuming the interference power remains constant for each path, the ideal SNR is,

$$SNR_{ideal} = \sum_{j=1}^{L} SNR_{ij} \tag{5.44}$$

where SNR_{ij} is given by (5.39).

The probability of surviving to each depth level of the sequential test is given in Table 5.4.

The overall computational savings can be calculated by counting the number of operations (multiplications and additions) that are performed overall, and compared

Design Parameters	Designed values
Temporal SPRT parameter b	0.1
Spatial tree search thresholds	
κ_1	35.9
κ_2	40
κ_3	50
κ_4	60
κ_5	70

Table 5.1: Thresholds used for the conservative design (design#1).

Design Parameters	Designed values
Temporal SPRT parameter b	0.4
Spatial tree search thresholds	
κ_1	39
κ_2	50
κ_3	69
κ_4	95
κ_5	120

Table 5.2: Thresholds used for a lower complexity receiver design (design#2).

Design Parameters	Designed values
Temporal SPRT parameter b	0.7
Spatial tree search thresholds	
κ_1	42
κ_2	53
κ_3	77
κ_4	113
κ_5	140

Table 5.3: Thresholds used for an alternative lower complexity receiver design (design#3).

to exhaustive search. The savings over a full search and resulting SNR are tabulated in Table 5.5.

5.8.3 Theoretical Verification

The mean test length for a truncated SPRT test can be calculated by numerically performing the convolution given in (5.21). To perform the convolutions, we can use Simpson's Rule to evaluate the integrals numerically, and generate the conditional probability densities for each stage of the test.

The results in Table 5.6 show that the numerically calculated test length and the test length obtained from simulation match closely.

Depth Level	Tree Nodes	Design #1 (Table 5.1)	Design #2 (Table 5.2)	Design #3 (Table 5.3)
1	2	0.96	0.176	0.0614
2	4	0.95	0.174	0.0367
3	8	0.93	0.159	0.0364
4	16	0.82	0.083	0.030
5	32	0.34.3	0.0197	0.002

Table 5.4: Simulation probability of reaching a given depth level (spatial processing) when no signal is present.

The calculated probability of false alarm at each depth level of the spatial search for design #2 is compared to Monte Carlo simulations in Table 5.7.

The numerical calculations model the interference using a Gaussian approximation. The Gaussian approximation method uses the central limit theorem to approximate the sums of signals from interfering users as a Gaussian distribution. As the number of users increases, the accuracy of approximation also increases. By using the Gaussian approximation, we are introducing error in the model.

A theoretical value of the SNR can be calculated by finding the probability that a signal component will not be rejected. We can find the probability that a signal component is accepted by evaluating the probability of acceptance during the temporal and spatial search stages separately.

Design #	Savings	Resulting SNR (dB)
Ideal	0%	20.2
1	3%	20.1
2	84%	19.3
3	96.7%	18.87

Table 5.5: Resulting computational savings vs performance, of both spatial and temporal processing, in terms of output SNR.

For the temporal sequential testing stage, the SPRT designs a test that is conservative if the test was an untruncated SPRT. For an truncated SPRT, where the number of stages is finite, the design is only approximate. The probability of H_1 being accepted is:

$$Pr\{H_1 \text{ accepted}\} = \tag{5.45}$$

$$\int_{-T_c/2}^{T_c/2} \frac{1}{T_c} d\tau \int_0^\infty f_R(a_{ij}) da_{ij} \int_{b_G - a_{ij}}^\infty dx f_G\left(x|\lambda = a_{ij}\frac{T_c - 2|\tau|}{T_c}\right) \tag{5.46}$$

where $f_G(x|\lambda)$ is the distribution of the test statistic at the final stage of the sequential test with mean λ. The fading amplitude of each multipath is modeled using the Rayleigh distribution for $f_R(a_{ij})$.

For the spatial search stage, the probability of H_1 being accepted is given by (5.37), where averaging is performed over the random delay τ and fading amplitude a_{ij}.

These probabilities may either be calculated for particular values of a_{ij} or averaged

Design #	Simulation	Theoretical
Ideal	256	256
1	255	255
2	191	180
3	127	118

Table 5.6: Calculated and simulated test length for temporal sequential detection, rounded to the nearest integer.

over the probability distribution of a_{ij}.

The theoretical SNR, for RAKE combining, can be calculated by:

$$E\{SNR\} = \sum_{i=1}^{N}\sum_{j=1}^{L} E\{\frac{a_{ij}^2}{IN_{ij}} Pr\{H_1 \text{ accepted }\}\} \tag{5.47}$$

The theoretical SNR and simulated SNR are listed in Table 5.8.

From Table 5.8, we can conclude that the results obtained from simulation are very close to the results by evaluating evaluating (5.47) using numerical integration algorithm.

5.9 Conclusion

In this chapter, we have proposed a new sequential-detection based RAKE receiver which allows for the search of large space of possible parameters with reduced complexity compared to a full search, with only a slight degradation in output SNR.

Stage #	Simulation	Theoretical
1	0.18	0.17
2	0.176	0.158
3	0.158	0.150
4	0.083	0.076
5	0.019	0.012

Table 5.7: Theoretical and simulation probability reaching a given spatial tree depth level when no signal is present

By formulating a hypothesis test problem for each delay-sector parameter pair, we can detect whether multipath energy is present. By quickly rejecting paths with no energy, we can decrease the number of calculations needed by the RAKE receiver as compared to a "brute-force" full search. To detect whether a signal is present for a specific parameter pair, a sequential detector combined with a tree-structured spatial search is used to reduce the computational cost.

A SPRT was designed using Wald's approximation [32] for the temporal multipath detection. The tree-structured sequential spatial search was designed by finding thresholds that would satisfy a specific probability of detection using numerical calculation of resulting probability of detection. Simulations performed on 10 continuously transmitting users have demonstrated the reduced computation costs and corresponding output SNR performance of the RAKE receiver. A design was provided with an

Design #	Simulation (from Table 5.5)	Theoretical Eqn. (5.47)
1	20.1dB	20.0dB
2	19.3dB	19.4dB
3	18.9dB	18.3dB

Table 5.8: Theoretical and simulated output SNR from spatial and temporal processing.

84% reduction in multiplications and additions, and only a 0.9 dB penality in output SNR.

By using the framework presented in this chapter, we can more efficiently search over a large time interval in terms of the number of chips, and attempt to collect all the multipath energy in that interval. The structure was shown to significantly reduce the computational requirements of a RAKE receiver with only a small sacrifice in performance over that of a full search.

Chapter 6

Summary and Future Work

6.1 Summary

In this thesis, CDMA downlink and uplink base station processing is studied. In Chapter 3, an algorithm to perform beamforming for the downlink CDMA channel was presented. The algorithm contains three steps:

- Channel estimation using feedback from mobile with no pilot signal was presented for the downlink channel with multiple coherent antenna elements at the base station.
- Generation of directional beamforming weights using the results from channel estimation.
- Allocation of power to each user to maximize the SINR with different levels of quality of service.

In Chapter 4, the benefits of frequency re-use using the above algorithm was presented in a multi-cell multi-user environment. Inter-cell and intra-cell interference are approximated as additive white Gaussian noise. Inter-cell interference is caused by other base stations using the same frequency band and time slots. Intra-cell interference is caused by asynchronous reception due to scattering. The simulation results illustrate the benefits of downlink beamforming in terms of decreased cell density.

In Chapter 5, a new 2-D RAKE structure is proposed for use in uplink base station processing. A multiple element antenna array is used at the base station to allow for spatial processing. With a pre-generated set of weight vectors, the algorithm performs a full search of the parameter space by forming a hypothesis for each delay and weight vector, and detecting the presence of a signal for each parameter pair. By using a sequential detector and a tree-structured spatial search, we can reduce the computational cost of the search compared with "brute-force" full search.

6.2 Future Work

Future extensions of the research in the area of downlink beamforming in a CDMA environment could be,

- In the downlink CRV-based power control algorithm, a particular user's directional weight vectors were chosen independently of power allocation. Additional

research on joint optimization of directional weight vector and power allocation may yield improved capacity and cell coverage.

- The downlink channel estimation models the changes in the CRV as independent of the CRV itself. If research is performed on modeling the changes in CRV over time, one can derive a model for the Kalman filter "plant noise", and improve the estimator.

- For the uplink CDMA channel model, the fading experienced for each multipath component is based on the fading characteristic of the IS-95 channel. Additional research on the effect of reduced chip period in wideband CDMA on the fading characteristics of individual multipath signals would allow for more accurate performance analysis.

- Since the analysis (in Chapter 5.5.2) holds for non-Gaussian interference, a more detailed model of the interference can be developed and used for more accurate performance assessment.

6.3 Conclusion

In this thesis, a downlink CRV-based power control algorithm was presented. The CRV-based power control algorithm combines digital beamforming and power control to increase coverage and capacity of the downlink in a DS-CDMA system. The CRV-based power control algorithm contains three parts, MMSE channel estimation, digital

beamforming, and optimum intra-cell power allocation method. Simulation results for a multi-cell multi-user DS-CDMA environment was presented in the presence of inter-cell and intra-cell interference.

The second contribution of this thesis is a proposed computationally efficient wide-band spatial-temporal RAKE receiver structure. A SPRT test is proposed to perform the spatial search for multipath signal. For spatial search of the multipath signal, a test performance analysis was developed and used to determine the decision thresholds for a tree-structured search. The proposed structure comprised of a sequential detection stage followed by a tree-structured spatial search stage. The structure allows for a more efficient spatial-temporal search for the presence multipath signal. The algorithm can offer significant reduction in computational cost as compared to a "brute-force" full search of the same search space with only a modest performance penalty.

Bibliography

[1] Adachi, F., Sawahashi, M., and Suda, H., "Wideband DS-CDMA for Next-Generation Mobile Communications Systems," *IEEE Communications Magazine*, Sept. 1998 pp56-69

[2] Aue, V., and Fettweis, G., "A Non-Coherent Tracking Scheme for the RAKE Receiver That Can Cope With Unresolvable Multipath," Proceedings of ICC'99, S48-2

[3] Bar-Shalom, Y., and Fortmann, T. E., *Tracking and Data Association*, Academic Press Inc., San Diego, 1988

[4] Blostein, S. D., and Huang, T. S., "Detecting Small, Moving Objects in Image Sequences Using Sequential Hypothesis Testing," *IEEE Transactions on Signal Processing*, Vol. 39, No 7, July 1991, pp 1611-1629

[5] Brennan, D. G., "Linear Diversity Combining Techniques", Proceedings of the IRE, vol. 47, pp. 1075-1102, 1959

[6] Capon, J., "High resolution frequency-wavenumber spectrum analysis," Proc. IEEE, vol. 57, pp.1408-1418, Aug. 1969

[7] Cheun, K., "Performance of Direct-Sequence Spread-Spectrum RAKE Receivers with Random Spreading Sequences," *IEEE Transaction on Communications*, Vol 45, No 9, Sept., 1997

[8] Colman, G., *An Investigation Into The Capacity of Cellular CDMA Communication Systems With Beamforming In Environments with Scatter*, M.Sc. Thesis, Queen's University, Sept. 1998.

[9] Dahlman, E., Gudmundson, B., Nilsson, M., and Skold, J., "UMTS/IMT-2000 Based on Wideband CDMA," *IEEE Communications Magazine*, Sept. 1998, pp 70-80

[10] Dinan, E. H., and Jabbari, B., "Spreading Codes for Direct Sequence CDMA and Wideband CDMA Cellular Networks," *IEEE Communications Magazine*, Sept. 1998, pp 48-54

[11] Earnshaw, M., *An investigation into Improving Performance of Cellular CDMA Communication Systems with Digital Beamforming*, PhD Thesis, Queen's University, Aug. 1997

[12] Rashid-Farrokhi, F., Liu, K. J. R., and Tassiulas, L., "Downlink Power Control and Base Station Assignment," *IEEE Communications Letters*, Vol. 1, No. 4, July 1998, pp150-152

[13] Gerlach, D., and Paulraj, A., "Adaptive Transmitting Antenna Arrays with Feedback," *IEEE Signal Processing Letters*, Vol 1, No. 10, Oct. , 1994

[14] Gilhousen, K. S., Jacobs, I. M., Padovani, R., Viterbi, A. J., Weaver Jr., L., and Wheatley III, C., "On the Capacity of a Cellular CDMA System," *IEEE Transactions on Vehicular Technology*, Vol 40, No. 2, May, 1991, pp303-312

[15] Hosangadi, G. S., and Baum C. W., "Hybrid Sequential Acquisition Schemes for Noncoherent Chip-Asynchronous DS/SS Systems", ICC '99 Proceedings, S30-8

[16] Jalali, A., and Gutierrez, A., "Performance Comparison of Direct Spread and Multicarrier CDMA Systems,"VTC '98 Proceedings, pp2042-2046

[17] Kansal, A., Batalama, S., Pados, D. A. P., "Adaptive Maximum SINR RAKE Filtering for DS-CDMA Multipath Fading Channels," *IEEE Journal on Selected Areas in Communications*, Vol. 16, No. 9, December 1998, pp 1765-1773

[18] Kim, C. K., and Cho, Y. S., "Capacity Improvement of a MC-CDMA Cellular System with Antenna Arrays in a Fading Channel," VTC '98 Proceedings, pp 2032-1248

[19] Kim, D., "Downlink Power Allocation and Adjustment for CDMA Cellular Systems," *IEEE Communications Letters*, Vol. 1, No. 4, July 1998

[20] Kondo, S., and Milstein, L. B., "Performance of Multicarrier DS CDMA System," *IEEE Transaction on Communications* Vol 44, No. 2, Feb. 1996

[21] Liu, H., Xu, G., "Smart Antennas in Wireless Systems: Uplink Multiuser Blind Channel and Sequence Detection," *IEEE Transactions on Communications*, Vol45, No. 2, Feb. 1997

[22] Liu, H., Zoltowski, M. D., "Blind Equalization in Antenna Array CDMA Systems", *IEEE Transactions on Signal Processing*, Vol 45, No 1, Jan. 1997

[23] Naguib, Ayman F., "Adaptive Antennas for CDMA Wireless Networks," Ph.D. dissertation, Stanford, August 1996

[24] Naguib, A.F., Paulraj, A., Kailath, T., "Capacity improvement with base-station antenna arrays in cellular CDMA," *IEEE Transaction on Vehicular Tecnology*, Vol. 43, No. 3, pp691-698, 1994

[25] Ogawa, Y., Sasaki, R., Ohgane, T., and Itoh, K., "An Adaptive Antenna for a Multipath Propagation Environment," Proceedings of VTC '98, pp544-548

[26] Ojanpera, T., and Prasad, R., "An Overview of Air Interface Multiple Access for IMT-2000/UMTS," *IEEE Communications Magazine*, Sept. 1998, pp82-95

[27] Okawa, K., Okumura, Y., Sawahashi, M., and Adachi, F., "1.92 Mbps data transmission experiments over a coherent W-CDMA mobile radio link", VTC '98 Conference Proceedings, pp1300-1304

[28] Papoulis, A., *Probability, Random Variables, and Stochastic Processes,* 3rd Ed., McGraw-Hill, Toronto, 1991

[29] Paulraj, A. J., and Papdias, C., "Space-Time Processing for Wireless Communications," IEEE Signal Processing Magazine, Nov., 1997

[30] Pillai, S. U., *Array Signal Processing,* Springer-Verlag, New York, 1989

[31] Polydoros, A., Weber, C. L., "A Unified Approach to Serial Search Spread-Spectrum Code Acquisition - Part I: General Theory," *IEEE Transactions on Communications*, Vol. COM-32, No 5, May 1984

[32] Poor, H. V., *An Introduction to Signal Detection and Estimation,* Springer-Verlag, New York, 1994

[33] Proakis, J. G., *Digital Communications,* 3rd ed., McGraw-Hill, Toronto, 1995

[34] Qualcomm, *http://www.qualcomm.com/technology*

[35] Rappaport, T. S., *Wireless Communications - Principles & Practices*, Prentice-Hall, Toronto, 1996

[36] Raleigh, G. G., and Boros, T., "Joint Space-Time Parameter Estimation for Wireless Communication Channels", *IEEE Transaction on Signal Processing*, Vol. 46, No. 5, May 1998, pp. 1333-1343

[37] Rezeanu, S., Ziemer, R. E., and Wickert M. A., "Join Maximum-Likelihood Parameter Estimation for Burst DS Spread-Spectrum Transmission," *IEEE Transactions on Communications*, Vol. 45, No. 2, Feb., 1997

[38] Sathyendran, A., Sowerby, K. W., Shafi, M., "A Statistical Approach to the Analysis of DS/CDMA Cellular System Employing RAKE receivers," IEEE Transaction on Vehicular Technology, Vol. 48, No. 1, Jan. 1999

[39] Simon, M. K., Omura, J. K., Scholtz, R. A. and Levitt, B. K., *Spread Spectrum Communication Vol. III*, Computer Science Press, Rockville, 1985

[40] Sundelin, M., Granzow, W., and Olofsson, H., "A Test System for Evaluation of the WCDMA Technology," VTC '98 Proceedings, pp 983-987

[41] Tantaratana, S., Poor, H. V., "Asymptotic relative efficiencies of multistage tests," *IEEE Transactions on Information Theory*, vol. IT-28, no. 6, pp911-923, 1982

[42] Tantaratana, S., Lam, A. W., Vincent, P. J., "Noncoherent Sequential Acquisition of PN sequences for DS/SS Communications with/without Channel Fading," *IEEE Transactions on Communications*, Vol. 43, No. 2/3/4, Feb/Mar/Apr 1995

[43] Tao, L, *Beamforming in the Uplink and Downlink Channels of a Cellular CDMA Communication System*, M.Sc. Thesis, Feb., 1998

[44] van der Veen, A., Vanderveen, M. C., and Paulraj, A., "Joint Angle and Delay Estimation Using Shift-Invariance Techniques," *IEEE Transactions on Signal Processing*, Vol. 46, No. 2, Feb., 1998,

[45] Wald, A., *A., Sequential Analysis* New York: Wiley, 1947

[46] Wald, A., Wolfowitze, J. , "Optimum Character of the Sequential Probability Ratio Test," *Ann. Math. Statist.*, Vol. 19, p. 326, 1948

[47] Wang, X., Poor, H. V., "Blind Equalization and Multiuser Detection in Dispersive CDMA Channels," *IEEE Transaction on Communications*, Vol 46, No 1, Jan., 1998

[48] Wax, M., Leshem, A., "Joint Estimation of Time Delays and Directions of Arrival of Multiple Reflections of a Known Signal", *IEEE Transactions on Signal Processing*, Vol. 45, No 10, Oct 1997, pp 2477-2482

[49] Weiss, A. J., Friedlander, B., "Synchronous DS-CDMA Downlink with Frequency Selective Fading," *IEEE Transacation on Signal Processing*, Vol. 47, No. 1, Jan. 1999

[50] Win, M. Z., Chrisikos, G., and Sollenberger, N. R., "Impact of Spreading Bandwidth and Diversity Order on the Error Probability Performance of Rake Reception in Dense Multipath Channels" WCNC '99 Conference Proceedings , Sept. 1999

[51] Yang, W., and Xu, G. "The optimal Power Assignment for Smart Antenna Downlink Weighting Vector Design," VTC '98 Conference Proceedings, pp485-488.

[52] Ziemer, R. E. and Peterson, R. L., *Digital Communications and Spread Spectrum Systems*, Macmillan Publishing Company, New York, 1985

Vita

Li Yang Pan

EDUCATION

Queen's University	M.Sc.	Electrical and Computer Engineering	1997–99
Queen's University	B.Sc.Eng	Electrical and Computer Engineering	1993–97

EXPERIENCE

Member of Technical Staff (1999–),

Baseband DSP Engineer

Nokia Mobile Phone, San Diego, CA

Research Assistant (1997–1999),

Electrical and Computer Engineering, Queen's University

Summer Research Assistant (1996,1997),

Electrical and Computer Engineering, Queen's University